Oxysterol-Induced Soluble Endoglin Release and Its Involvement in Hypertension

Ana C. Valbuena-Diez, MSc; Francisco J. Blanco, PhD; Barbara Oujo, MSc; Carmen Langa, BSc; María Gonzalez-Nuñez, MSc; Elena Llano, PhD; Alberto M. Pendas, PhD; Mercedes Díaz, BSc; Antonio Castrillo, PhD; José M. Lopez-Novoa, PhD; Carmelo Bernabeu, PhD

Background—Ischemia in the placenta is considered the base of the pathogenesis of preeclampsia, a pregnancy-specific syndrome in which soluble endoglin (sEng) is a prognostic marker and plays a pathogenic role. Here, we investigated the effects of hypoxia and the downstream pathways in the release of sEng.

Methods and Results—Under hypoxic conditions, the trophoblast-like cell line JAR showed an increase in sEng parallel to an elevated formation of reactive oxygen species. Because reactive oxygen species are related to the formation of oxysterols, we assessed the effect of 22-(R)-hydroxycholesterol, a natural ligand of the liver X receptor (LXR), and the LXR synthetic agonist T0901317. Treatment of JAR cells or human placental explants with 22-(R)-hydroxycholesterol or T0901317 resulted in a clear increase in sEng that was dependent on LXR. These LXR agonists induced an increased matrix metalloproteinase-14 expression and activity and a significant reduction of its endogenous inhibitor, tissue inhibitor of metalloproteinase-3. In addition, mice treated with LXR agonists underwent an increase in the plasma sEng levels, concomitant with an increase in arterial pressure. Moreover, transgenic mice overexpressing sEng displayed high blood pressure. Finally, administration of an endoglin peptide containing the consensus matrix metalloproteinase-14 cleavage site G-L prevented the oxysterol-dependent increase in arterial pressure and sEng levels in mice.

Conclusions—These studies provide a clue to the involvement of the LXR pathway in sEng release and its pathogenic role in vascular disorders such as preeclampsia. **(*Circulation*. 2012;126:2612-2624.)**

Key Words: cell hypoxia ■ hypertension ■ pre-eclampsia ■ pregnancy ■ peptides

Preeclampsia is a pregnancy-specific syndrome characterized by systemic hypertension, proteinuria, and edema in the third trimester of pregnancy.[1,2] It affects both the fetus and the mother and occurs in ≈5% of pregnancies. Severe preeclampsia leads to the appearance of the HELLP syndrome (hemolysis, elevated liver enzymes, and low platelets), seizures, or fetal growth restriction and can result in fetal death. Preeclampsia is thought to be the consequence of impaired placentation resulting from inadequate trophoblastic invasion of the maternal spiral arteries.[3] Abnormal placentation is an important predisposing factor for preeclampsia, whereas endothelial dysfunction appears to be central to the pathophysiological changes, possibly indicative of a 2-stage disorder characterized by reduced placental perfusion and a maternal syndrome. Hypoxia, followed by oxidative stress, has been postulated as a critical signal that initiates the pathogenic process in preeclampsia.[4,5] Hypoxia and extracellular inflammatory signals can induce the intracellular accumulation of reactive oxygen species (ROS).[6,7] In turn, the imbalance between ROS production and antioxidant systems induces oxidative stress that negatively affects reproductive processes, including cyclic luteal and endometrial changes, follicular development, ovulation, fertilization, embryogenesis, embryonic implantation, and placental differentiation and growth.[5] ROS-induced damage can target lipids, proteins, and DNA. In this context, endogenously oxygenated cholesterol derivatives (oxysterols) such as 24(S)-hydroxycholesterol and 22(R)-hydroxycholesterol (22-R) were identified as endogenous agonists of liver X receptors (LXRs).[8,9] Many different oxysterols are known, and they all share a cholesterol structure with an oxygen-containing functional group such as alcohol, carbonyl, or epoxide.[10] The wide array of

Received February 22, 2012; accepted October 19, 2012.

From the Centro de Investigaciones Biológicas, Consejo Superior de Investigaciones Científicas (CSIC), and Centro de Investigación Biomédica en Red de Enfermedades Raras (CIBERER), Madrid (A.C.V.-D., F.J.B., C.L., C.B.); Unidad de Fisiopatología Renal y Cardiovascular, Departamento de Fisiología y Farmacología, Universidad de Salamanca (USAL), Campus Miguel de Unamuno and Instituto de Investigación Biomédica de Salamanca (IBSAL), Salamanca (B.O., M.G.-N., E.L., J.M.L.-N.); Centro de Investigación del Cancer (CSIC-USAL), Campus Miguel de Unamuno, Salamanca (E.L., A.M.P.); and Instituto de Investigaciones Biomédicas "Alberto Sols" CSIC-Universidad Autonoma de Madrid and Unidad Asociada de Biomedicina IIBM CSIC-Universidad de Las Palmas de Gran Canaria, Las Palmas de Gran Canaria (M.D., A.C.), Spain.

The online-only Data Supplement is available with this article at http://circ.ahajournals.org/lookup/suppl/doi:10.1161/CIRCULATIONAHA.112.101261/-/DC1.

Correspondence to Carmelo Bernabeu, PhD, Centro de Investigaciones Biológicas, c/Ramiro de Maeztu 9, Madrid 28040, Spain. E-mail bernabeu.c@cib.csic.es

Circulation **is available at http://circ.ahajournals.org** **DOI: 10.1161/CIRCULATIONAHA.112.101261**

oxysterols encountered in human health and disease vary in origin. Their oxygen-containing functional group can be added at the sterol ring or at the side chain of cholesterol by a nonenzymatic oxidation, an enzymatic oxidation, or both. Oxysterols play a role in many biological processes, including cholesterol homeostasis, sphingolipid metabolism, platelet aggregation, apoptosis, and protein prenylation. Oxysterols are modulators of cholesterol metabolism, ranging from regulation of cholesterol synthesis to regulation of cholesterol elimination through bile acid synthesis. They also have important implications in physiopathology and have been involved in atherosclerosis, thrombosis, or hypercholesterolemia, among others.[10,11] Moreover, oxysterols inhibit the differentiation and fusion of term primary trophoblasts by activating LXRs.[12]

Clinical Perspective on p 2624

LXRs are ligand-activated transcription factors that form heterodimers with the retinoic X receptor (RXR) that, on ligand binding, regulate the expression of different target genes.[13] LXRs are now considered "sterol sensors" because they regulate the expression of key gene products that control intracellular cholesterol homeostasis through catabolism and transport.[14–17] In addition to oxysterols, most studies on LXR activity have been validated with potent synthetic ligands such as the nonsteroidal Tularik agonist T0901317 (T09).[18] It has been reported that T09 acts selectively through LXR and in concert with its RXR heterodimerization partner.[19] Two variants of LXR, α and β, have been described.[16] Whereas LXR-α is highly expressed mainly in the liver, kidney, small intestine, adipose tissue, and macrophages, the presence of LXR-β is ubiquitous in most tissues.[20] Oxysterols are detected at relatively high levels in the placenta, and a role for LXRs in the reproductive system and a potential application of LXR agonists in the treatment of reproductive pathologies have been suggested.[15] In addition, LXR-α and LXR-β are expressed in human and mouse trophoblasts and the placenta from early gestation.[21,22] LXR isoforms have also been detected in several human trophoblast cell lines like JAR.[22,23] Of note, one of the LXR target genes is human endoglin (*ENG*), which contains 6 putative LXR response elements in its proximal promoter region, at least 1 of which binds the LXR/RXR heterodimer to stimulate transcription and total endoglin expression in response to 22-R, T0901317, or synthetic RXR agonists.[24]

The endothelial dysfunction in preeclampsia is thought to be caused by circulating factors that are released from the placenta. In preeclampsia, the maternal plasma concentration of free vascular endothelial growth factor and placental growth factor is decreased and the concentration of soluble fms-like tyrosine kinase-1 (sFlt-1) and soluble endoglin (sEng) is increased.[2] A pathogenic role for sEng has been reported,[25,26] and there is a growing interest in elucidating the regulated expression and role of this potential therapeutic target in preeclampsia.[27] Interestingly, sera from pregnant women with preeclampsia can upregulate the levels of endoglin mRNA and induce the release of sEng in choriocarcinoma cells.[28] Endoglin is a transmembrane auxiliary receptor for transforming growth factor-β that modulates cellular responses to multiple members of the transforming growth factor-β family.[29] Endoglin is highly expressed on proliferating endothelial cells and syncytiotrophoblasts, including the trophoblast cell line JAR,[29–31] and regulates trophoblast differentiation along the invasive pathway in human placental villous explants.[32] Of note, sEng, generated by proteolytic shedding, antagonizes the membrane-bound form.[25,33,34]

Here, we show that the hypoxia-induced pathway involving ROS and oxysterols activates the proteolytic release of sEng, a process that can be blocked in vitro and in vivo by endoglin-related peptides carrying a matrix metalloproteinase-14 (MMP-14) cleavage site. Moreover, mice treated with either oxysterols or LXR agonists underwent an increase in plasma sEng levels, concomitant with an increase in arterial pressure. An increase in arterial pressure was also observed in mice overexpressing MMP-14 that showed high levels of plasma sEng, supporting a role of the LXR pathway in the sEng release and its contribution to vascular homeostasis regulation.

Methods

Cell and Tissue Culture

The human placental choriocarcinoma cell line JAR,[31] human umbilical vein endothelial cells (Lonza, Walkersville, MD), and stable transfectants of rat myoblast L6E9[35] and mouse fibroblast L929[36] expressing human endoglin were grown as described. Mouse embryonic fibroblasts from wild-type (WT) and LXR knockout ($Lxr\alpha,\beta^{-/-}$) mice and monkey kidney COS-7 cells were grown in Dulbecco modified Eagle medium. For LXR activation studies, cells were incubated with T0901317 (Calbiochem), 22-R, or 9-cis-retinoic acid (RA; Sigma-Aldrich, L'Isle D'Abeau, France). For metalloprotease inhibition assays, cells were incubated with recombinant human tissue inhibitor of metalloproteinase (TIMP)-1, -2, or -3 (R&D Systems, Minneapolis, MN), doxycyclin (Sigma-Aldrich) or endoglin peptides. For hypoxia treatments, JAR cells were incubated with 1% O_2 or in the presence of 100 μmol/L deferoxiamine mesylate salt (Sigma-Aldrich). Human fresh placental explants were collected in the delivery room of the University Hospital, Salamanca Spain, within 30 minutes of delivery from patients without complications. After removal of decidua and large vessels, 0.5 g tissue was cultured in complete Dulbecco modified Eagle medium–F12 medium. Explants were incubated for 24 hours with 5 μmol/L 22-R or 15 μmol/L endoglin peptides as indicated.

Plasmids and Cell Transfections

Expression vector encoding HA-tagged human endoglin in pDisplay has been described.[37] Expression vector encoding human MMP-14 was kindly provided by Dr Alicia Garcia-Arroyo (Centro Nacional Investigaciones Cardiovasculares, Madrid, Spain). Cell transfections were carried out with SuperFect Reagent (Qiagen, Crawley, UK).

Flow Cytometry

Immunofluorescence flow cytometry studies were carried out with primary monoclonal antibodies mouse anti-endoglin P4A4 and rabbit anti–MMP-14 (Abcam, Cambridge, UK), as well as with Alexa 488 anti-mouse or Alexa 647 anti-rabbit secondary antibodies.[37] For ROS detection analyses, JAR cells were subjected to hypoxia/normoxia in the presence of Trolox (Calbiochem) and incubated with 2′,7′-dichlorodihydrofluorescein diacetate (CM-H2DCFDA; Invitrogen, Carlsbad, CA), and their fluorescence was estimated.

ELISA Analysis

Concentrations of human sEng were determined by Quantikine Human Endoglin/CD105 (R&D Systems). The plasma concentra-

tions of mouse sEng were determined by DuoSet mouse endoglin/CD105 (R&D Systems). Concentrations of TIMP-3 were determined with a TIMP-3 human ELISA kit (Abnova, Taiwan). All immunoassays were measured in a Varioskan Flash spectral scanning multimode reader (Thermo Scientific).

Lipid Analysis and Liposome Preparation

Lipid extraction from adherent JAR cells was carried out according to the method of Bligh and Dyer[38] in a chloroform/methanol mixture. Lipids were derivatized to trimethylsilyl ethers with bis(trimethylsilyl)trifluoroacetamide and submitted to gas chromatography–mass spectrometry analysis (Agilent 7890A; Agilent Technologies). As control markers, purified cholesterol and 22-R were used. Liposomes containing L-α-phosphatidylcholine (Sigma) and 22-R were prepared at a molar ratio of 2:1 in PBS. When necessary, endoglin peptides were added to the mixture. The aqueous suspension was bath-sonicated for 1 hour before injection into mice.

Real-Time and Semiquantitative Reverse Transcriptase–Polymerase Chain Reaction Analysis of mRNA Levels

Total RNA was isolated from cells with the RNeasy kit (Qiagen) and reverse-transcribed with iScript cDNA Synthesis kit (Bio-Rad Laboratories, Hercules, CA). The resultant cDNA was used as a template for real-time polymerase chain reaction with the iQ SyBR-Green Supermix (Bio-Rad). Amplicons were detected with an iQ5 real-time detection system. For semiquantitative reverse transcriptase–PCT (RT-PCR), cDNA was subjected to PCR amplification with the HotMaster Taq DNA polymerase kit (5 Prime Inc, Gaithersburg, MD) with human TIMP-2, TIMP-3, and glyceraldehyde-3-phosphate dehydrogenase primers. PCR products were separated by agarose gel electrophoresis and documented in a Gel Doc XR System (Bio-Rad, Hercules, CA), and bands were quantified with the use of Quantity One software.

RNA Interference Experiments

The human small interfering ribonucleic acids (siRNA) for TIMP-3, hypoxia-inducible factor-1α, and scrambled siRNA were from Ambion Inc (Austin, TX). JAR cells were transfected with siRNA with lipofectamine 2000 (Invitrogen).

Metalloproteinase Activity

The metalloproteinase activity of JAR cells or placental explants was determined with the fluorogenic peptide Mca-PLGL-Dpa-AR-NH2 (R&D Systems). For cell-free assays, recombinant human MMP-14 (Millipore) was activated by incubation with 4-aminophenylmercuric acetate (Sigma). When necessary, the metalloproteinase activity was determined in the presence of 30 μmol/L endoglin peptides or 50 μmol/L doxycyclin.

Endoglin Peptides and Recombinant Protein

Short endoglin-related peptides P583 (TSKGLVLP), P447 (SLSFQLGLYL), and P230 (GPRTVTVK) with N-terminal acetylation and C-terminal amidation were synthesized and purified to >90% purity (Biomedal SL, Sevilla, Spain). Recombinant human endoglin encoding the extracellular domain (Glu26-Gly586) was purchased from R&D Systems Inc.

Mice and In Vivo Experiments

Mice from the C57BL/6J strain (male; age, 8–12 weeks) were infused intraperitoneally with T09 (40–50 mg/kg), 22-R (40–50 mg/kg), or vehicle alone (ethanol-saline solution 1:1) daily during 4 to 6 days. Alternatively, male or pregnant female (20 weeks old, third week of gestation) mice were intravenously injected in the tail vein with a liposome mixture containing 22-R (40–50 mg/kg) and L-α-phosphatidylcholine at a molar ratio of 1:2 in the presence or absence of 60 μg peptides per 1 g body weight per day. To upregulate in a tetracycline-dependent manner the endogenous MMP-14, Ola129/C57BL/6J knock-in mice were generated. A regulatory cassette was inserted immediately upstream of its translation initiation codon so that gene expression could be regulated by dietary doxycycline administration. Recombinant clones of embryonic stem cells containing the MMP-14 regulatory cassette were used to generate germline-transmitting chimeras by aggregation in morulas. Chimeric mice were bred with C57BL/6J females, and genotypes were determined by Southern blot analysis of tail DNA. Upregulation of MMP-14 was induced when mice were 5 weeks old. To generate transgenic mice expressing sEng (*Sol.eng*$^+$), a truncated endoglin construct (amino acids 26–437) driven by a ubiquitous actin promoter was microinjected into CBAxC57BL/6J fertilized eggs. Progeny was screened for endoglin transgene by PCR analysis of tail DNA. Studies reported here were performed in the F7 generation. The concentration of total protein in urine was measured by a colorimetric assay (Bradford Method). Systolic arterial pressure was measured in conscious mice with a tail cuff sphygmomanometer (NIPREM 546) equipment; in conscious, freely moving mice by radiotelemetry using a catheter implanted into an artery of the mouse attached to an implantable microminiaturized monitor (PA-C20, Data Sciences Intl); or in anesthetized mice using an intracarotid cannula connected to a blood pressure transducer. All of the experiments were approved by the appropriate institutional animal care and use committees.

Statistics

Data were subjected to statistical analysis, and results are shown as mean±SEM. Differences in mean values between 2 groups were analyzed with the Student *t* test (unpaired). Comparisons of several groups were done by 1-way (a single variable) or 2-way (two variables) ANOVA. Then, a posteriori *t* test was used for group comparisons (GraphPad Software). Additional information is given in the online-only Data Supplement.

Results

Hypoxia Induces sEng Shedding

Because hypoxia is a key event in the development of preeclampsia [1,2,4] and the increase of sEng is a prognosis marker for this pathology,[25] we assessed whether hypoxia is involved in the sEng release to the media. Thus, JAR cells were either incubated under 1% oxygen or treated with deferoxiamine mesylate salt for 24 hours. Then, conditioned media were collected and analyzed by ELISA. As shown in Figure 1A, both types of hypoxic stimuli significantly induced the shedding of sEng to the media. Similarly, sEng was increased in supernatants from either myoblast or fibroblast stable transfectants expressing endoglin when submitted to hypoxia (Figure 1B). Because the expression of human endoglin cDNA in these cell transfectants is driven by a viral promoter, these results exclude the possibility of a transcriptional regulation or an alternative splicing event and strongly suggest the existence of a proteolytic mechanism in the sEng formation during hypoxia. That hypoxia is involved in sEng release was further supported by RNA depletion studies of hypoxia-inducible factor-1α, a downstream component of the hypoxia pathway. Thus, siRNA-mediated knockdown of hypoxia-inducible factor-1α was carried out in JAR cells, subjected or not subjected to hypoxia, using 3 different siRNAs, and silencing of hypoxia-inducible factor-1α was monitored by quantitative RT-PCR (Figure 1C). Analysis by ELISA of the corresponding cell supernatants shows a marked decrease in the hypoxia-induced upregulation of sEng (Figure 1D).

There is increasing evidence that the high levels of sEng in preeclampsia are associated with both increased oxidative stress and reduced antioxidant defenses.[2,5] Thus, we wondered whether hypoxia was able to promote not only the

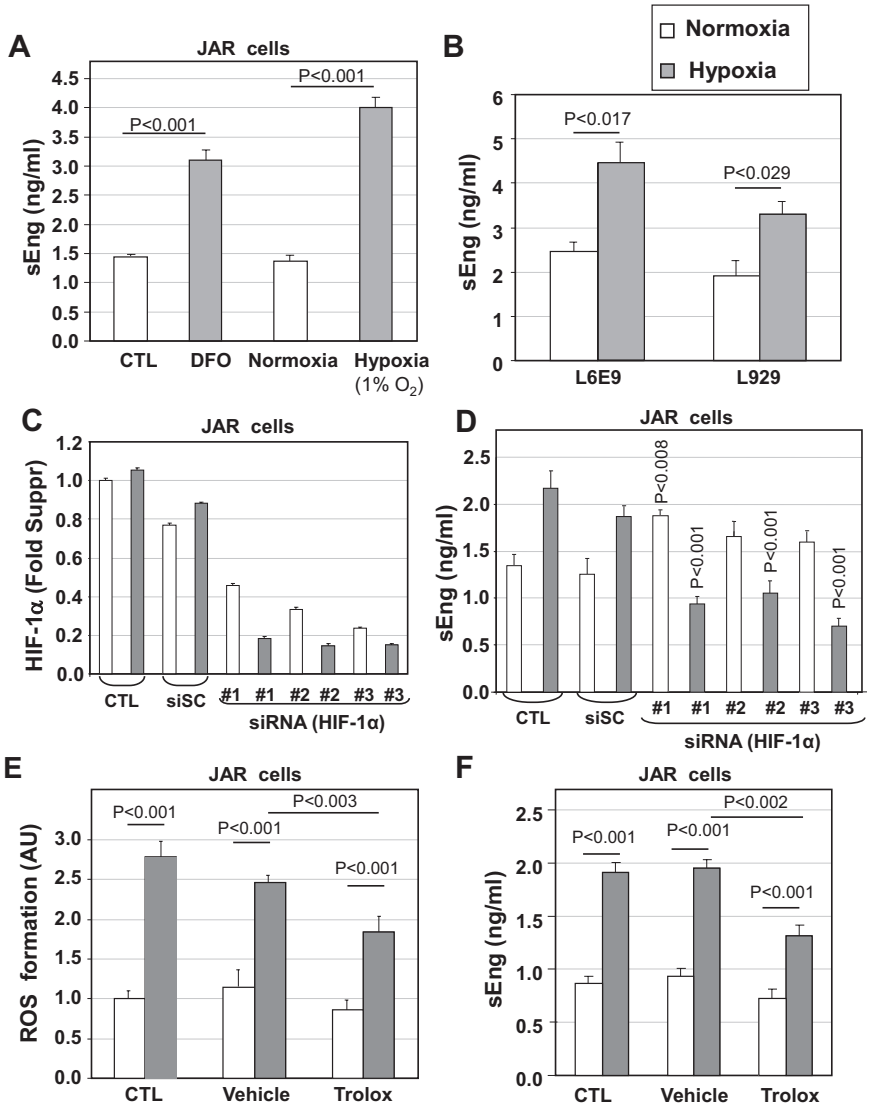

Figure 1. Effect of hypoxia on soluble endoglin (sEng) release. **A**, JAR cells were incubated with deferoxiamine mesylate salt (DFO) or 1% oxygen for 24 hours, and sEng levels were measured by ELISA (n=3 in each group). **B**, Rat myoblast (L6E9) and mouse fibroblast (L929) stable transfectants expressing human endoglin were incubated under hypoxic conditions (1% oxygen) for 24 hours, and sEng levels were measured by ELISA (n=3 in each group). **C** and **D**, JAR cells were transfected with 3 different small interfering RNA (siRNA) to silence *HIF-1α*. After 24 hours, real-time reverse transcriptase–polymerase chain reaction was used to measure hypoxia-inducible factor-1α (HIF-1α) expression (**C**), whereas sEng levels were determined by ELISA (**D**). Untreated control cells (CTL) and cells transfected with scrambled siRNA (siSC) are included. Statistical analyses of siRNA samples compared with CTL are indicated (siRNA#1 vs siSC under normoxia; siRNA#1, #2, and #3 vs siSC under hypoxia; n=3 in each group). **E** and **F**, JAR cells were subjected to hypoxic conditions (1% oxygen) either in the presence or in the absence of the antioxidant Trolox. After 24 hours, media were removed and sEng levels were measured by ELISA (**F**). Then, cells were incubated with 2′,7′-dichlorodihydrofluorescein diacetate (CM-H2DCFDA), a cell-permeant indicator for reactive oxygen species (ROS), and their fluorescence was analyzed by flow cytometry to determine the levels of ROS formation (**E**; n=3 in each group).

shedding of sEng but also the formation of ROS in JAR cells. Thus, JAR cells were submitted to hypoxia for 24 hours and then incubated with the ROS reactive probe CM-H2DCFDA. As evidenced by flow cytometry, ROS formation was induced in hypoxic JAR cells (Figure 1E). Moreover, this increase in the ROS formation was significantly blocked by treatment with Trolox, a potent antioxidant derived from vitamin E (Figure 1E). Interestingly, Trolox also induced a clear reduction in the sEng levels shed under hypoxic conditions (Figure 1F). These results suggest that ROS are a downstream component of the hypoxia pathway that leads to an increase of sEng.

Oxysterols Are Involved in the Shedding of sEng via the LXR Pathway

One of the effects of hypoxia-induced ROS in the cell is the generation of oxysterols.[39] Indeed, JAR cells subjected to hypoxia showed an increased production of 22-R compared with normoxic cells (Figure I in the online-only Data Supplement). Because oxysterols signal through the LXR receptors[17] and total endoglin expression is induced by the activation of the LXR pathway mediated by the LXR synthetic agonist T09,[24] we assessed the involvement of this pathway in the production of sEng. As expected, the treatment of JAR cells with T09 resulted in a clear increase in cell surface endoglin (Figure II in the online-only Data Supplement). In addition, treatment with T09, as well as with the physiological LXR ligand, the oxysterol 22-R, and the RXR ligand RA, induced a potent release of sEng (Figure 2A). Interestingly, 22-R and RA showed a positive synergistic cooperation in the release of sEng levels. Moreover, when primary cultures of human endothelial cells treated with the synthetic LXR agonist T09 were used, a clear upregulation of sEng levels was observed (Figure 2B). That the pathway of the nuclear receptor LXR is involved in sEng shedding was confirmed with the use of mouse embryonic fibroblasts derived from $Lxr\alpha,\beta^{-/-}$ double-knockout mice. On transfection with human endoglin, WT mouse embryonic fibroblasts showed an increased shedding of sEng in the presence of T09, whereas $Lxr\alpha,\beta^{(-/-)}$ mouse embryonic fibroblasts did not show any significant response to the LXR agonist (Figure 2C). Two different stable cell lines transfected with human endoglin

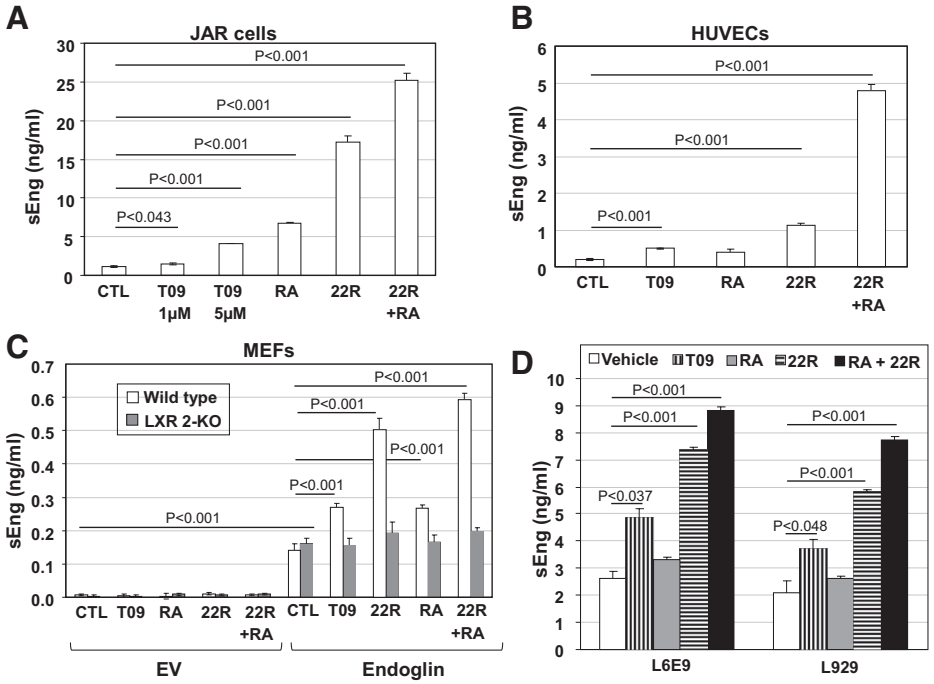

Figure 2. Effect of liver X receptor (LXR) ligands on soluble endoglin (sEng) production. Cells were treated with different combinations of T09, retinoic acid (RA), and 22(R)-hydroxycholesterol (22-R) for 24 hours as indicated, and sEng levels were measured in culture supernatants by ELISA. **A**, JAR cells. **B**, Human umbilical vein endothelial cells (HUVECs). Differences between every treatment compared with the control were analyzed by 1-way ANOVA and *t* test (**A** and **B**; n=3). **C**, Murine embryonic fibroblasts (MEFs) from wild-type (WT) or *LXRα,β* double-knockout (2-KO) mice were transfected with an expression vector encoding human endoglin or an empty vector (EV) before treatment with LXR ligands. Differences between WT and LXR 2-KO mock- and endoglin-transfected MEFs were analyzed with 2-way ANOVA, followed by *t* test; n=3. **D**, Rat myoblast (L6E9) and mouse fibroblast (L929) stable transfectants expressing human endoglin were incubated with LXR ligands as indicated (n=3). Statistical differences between each group and its control were assessed by 1-way ANOVA followed by *t* test.

cDNA displayed increased levels of sEng in the presence of T09 (Figure 2D). Because the expression of endoglin cDNA in these cells is driven by a potent viral promoter, these results exclude a possible transcriptional regulation in the generation of sEng and provide support for the proteolytic processing of the membrane-bound endoglin activated by the LXR pathway.

LXR Modulates the Proteolytic Cleavage of Endoglin Through the MMP-14 Inhibitor TIMP-3

Because MMP-14 mediates endoglin shedding[33] and the MMP-14 inhibitor TIMP-3 has been reported as a target gene of the LXR pathway,[40] we assessed whether TIMP-3 expression was modulated by hypoxia and LXR in JAR cells. As evidenced by quantitative RT-PCR, hypoxia markedly decreases mRNA levels of TIMP3 but leaves the transcript levels of TMP-2 unaffected (Figure 3A, left). Treatment with T09 leads to a significant reduction in TIMP-3 mRNA, as evidenced by semiquantitative RT-PCR (Figure 3A, right). In addition, TIMP-3 protein levels were downregulated in JAR cells treated with the LXR ligands T09 and 22-R (Figure 3B). To further confirm the involvement of TIMP-3, siRNA-mediated knockdown was carried out in JAR cells using 3 different siRNAs, and silencing of TIMP-3 was monitored by quantitative RT-PCR (Figure 3C). Analysis by ELISA of the corresponding conditioned supernatants shows an increase in sEng levels on TIMP-3 interference (Figure 3D). Conversely, incubation of JAR cells with recombinant human TIMP-3 showed a marked inhibition of the sEng levels induced by T09 (Figure 3E). In the same experiment, TIMP-1 showed a weak inhibitory effect, whereas TIMP-2 was able to reduce the levels of sEng greatly (Figure 3E), suggesting that the protease involved in the endoglin shedding is a common target for TIMP-3 and TIMP-2.

MMP-14 Is Involved in the Shedding of Endoglin in JAR Cells

TIMP-2 and TIMP-3 are inhibitors of MMP-14, which has recently been described as an endoglin-shedding protease in endothelial cells.[33] Therefore, we decided to study the role of MMP-14 in endoglin shedding from JAR cells. As shown in Figure 4A, sEng levels in the culture media from JAR cells overexpressing MMP-14 are significantly increased compared with controls. Similarly, coexpression of MMP-14 and human endoglin in COS-7 cells led to a clear increase in the levels of sEng (Figure 4B). Because T09 downregulates the MMP-14 inhibitor TIMP-3 (Figure 3), we next wondered whether the treatment of JAR cells with this LXR agonist increased the MMP-14 activity. To this end, we used the fluorogenic peptide Mca-PLGL-Dpa-AR-NH_2, which is specifically recognized as a substrate of MMP-14. As shown in Figure 4C, the MMP-14 activity was markedly enhanced in response to T09. As a control, this enhancement was abolished in the presence of doxycycline, a broad-spectrum protease inhibitor. Interestingly, the MMP-14 cleavage site G-L, present in the specific fluorogenic peptide, was identi-

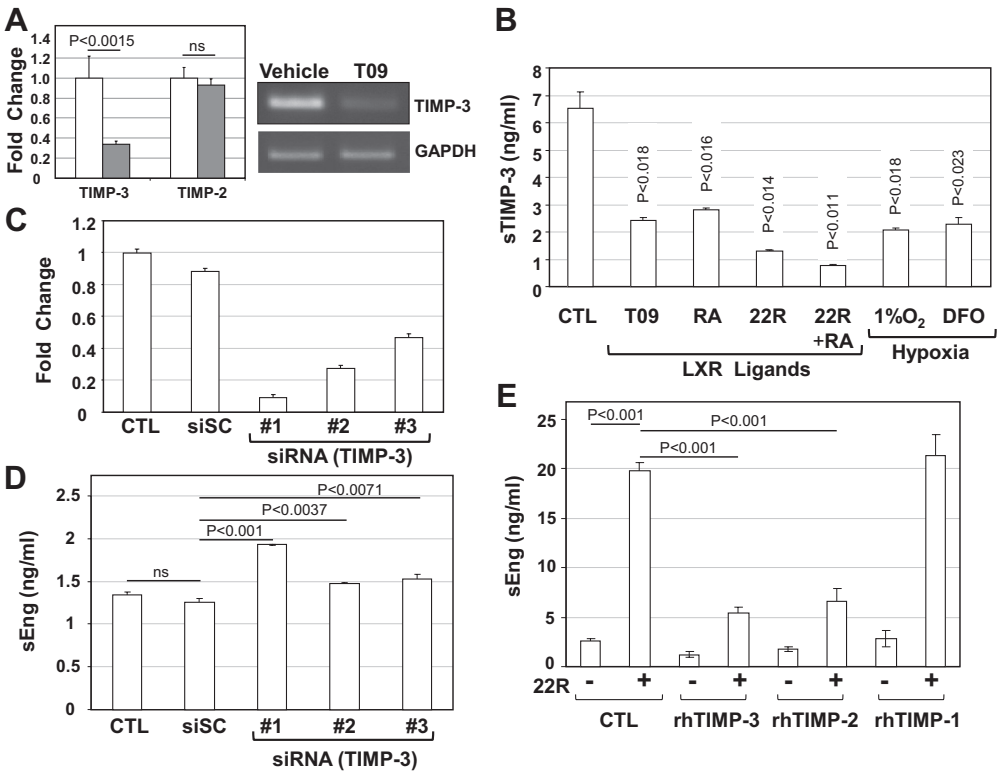

Figure 3. Involvement of tissue inhibitor of metalloproteinase (TIMP)-3 in the liver X receptor (LXR)/oxysterol pathway. **A**, Left, JAR cells were incubated under normoxia (□) or with 1% oxygen (■) for 24 hours, and TIMP-2 and TIMP-3 mRNA levels were measured by quantitative real-time reverse transcriptase–polymerase chain reaction (RT-PCR; n=3). Right, JAR cells were treated with T09 for 24 hours, and total RNA was extracted. Semiquantitative RT-PCR analysis shows that TIMP-3 mRNA levels are reduced after treatment. As a control, GAPDH mRNA levels were unchanged. Every treatment was compared with its control (n=3; *t* test). **B**, JAR cells were untreated (control [CTL]) or treated with T09, retinoic acid (RA), 22(R)-hydroxycholesterol (22-R), deferoxiamine mesylate salt (DFO), or 1% oxygen for 24 hours as indicated. The conditioned media were collected, and TIMP-3 levels were measured by ELISA. Every treatment was compared with the control (n=3; 1-way ANOVA followed by *t* test). **C** and **D**, JAR cells were transfected with 3 different small interfering RNA (siRNA) to silence TIMP-3. After 24 hours, real-time RT-PCR was used to measure TIMP-3 expression (**C**), whereas soluble endoglin (sEng) levels were determined by ELISA (**D**). A scrambled siRNA (siSC) was also transfected as a control (CTL vs siSC; siRNA#1, #2, and #3 vs siSC; n=3 in each group; 1-way ANOVA followed by *t* test). **E**, JAR cells were treated with recombinant TIMP-1, -2, and -3 proteins for 24 hours, and sEng levels were analyzed with ELISA (n=3 in each group; 1-way ANOVA followed by *t* test).

fied in 2 juxtamembrane peptides of the endoglin extracellular domain. This finding prompted us to postulate a possible modulatory effect of these peptides on endoglin shedding. For this purpose, 3 endoglin peptides were synthesized (Figure 4D). Incubation in a cell-free system of recombinant MMP-14 with a fluorogenic substrate in the presence of peptides P447 and P583 showed that these peptides, alone or combined, significantly inhibited MMP-14 activity, suggesting that these endoglin sequences are targets of MMP-14. As a negative control, incubation with the endoglin peptide P230, lacking the GL motif, did not affect the MMP-14 activity. Because peptide P583 showed the strongest inhibitory effect and the relative position of its cleavable GL motif fits well with the reported size of sEng,[33] it was selected for further studies. To assess whether peptide P583 could compete with the proteolytic processing of membrane-bound endoglin, sEng levels of JAR cells were measured in the presence of endoglin peptides. Peptide P583 but not P230 significantly inhibited the basal sEng shedding, suggesting that this endoglin sequence mimics the natural sequence of membrane-bound endoglin, interfering with the proteolytic activity of MMP-14 (Figure 4E). As a control, incubation with the protease inhibitor doxycycline rendered levels of inhibition similar to P583. Because MMP-14 activity is induced by LXR ligands (Figure 4C), we next assessed whether MMP-14 expression was also modulated by the LXR pathway. Indeed, incubation of JAR cells with different combinations of LXR ligands (T09, RA, and 22-R) and under hypoxic conditions resulted in an upregulated expression of the cell surface MMP-14 (Figure 4F and Figure III in the online-only Data Supplement). The effect of 22-R was also tested on human placental explants (Figure 4G–4I). In the presence of 22-R, sEng levels were significantly enhanced compared with controls, and this increase was inhibited by peptide P583 but not by P230 (Figure 4G). Similar to JAR cells, sEng levels paralleled MMP-14 activities in each treatment condition (Figure 4H), and soluble TIMP-3 levels were significantly inhibited in the presence of 22-R (Figure 4I) in human placental explants.

Activation of the LXR Pathway In Vivo Augments Serum Levels of sEng and Systolic Arterial Pressure

Next, we investigated whether our results with cultured cells could be reproduced in an animal model. To this purpose,

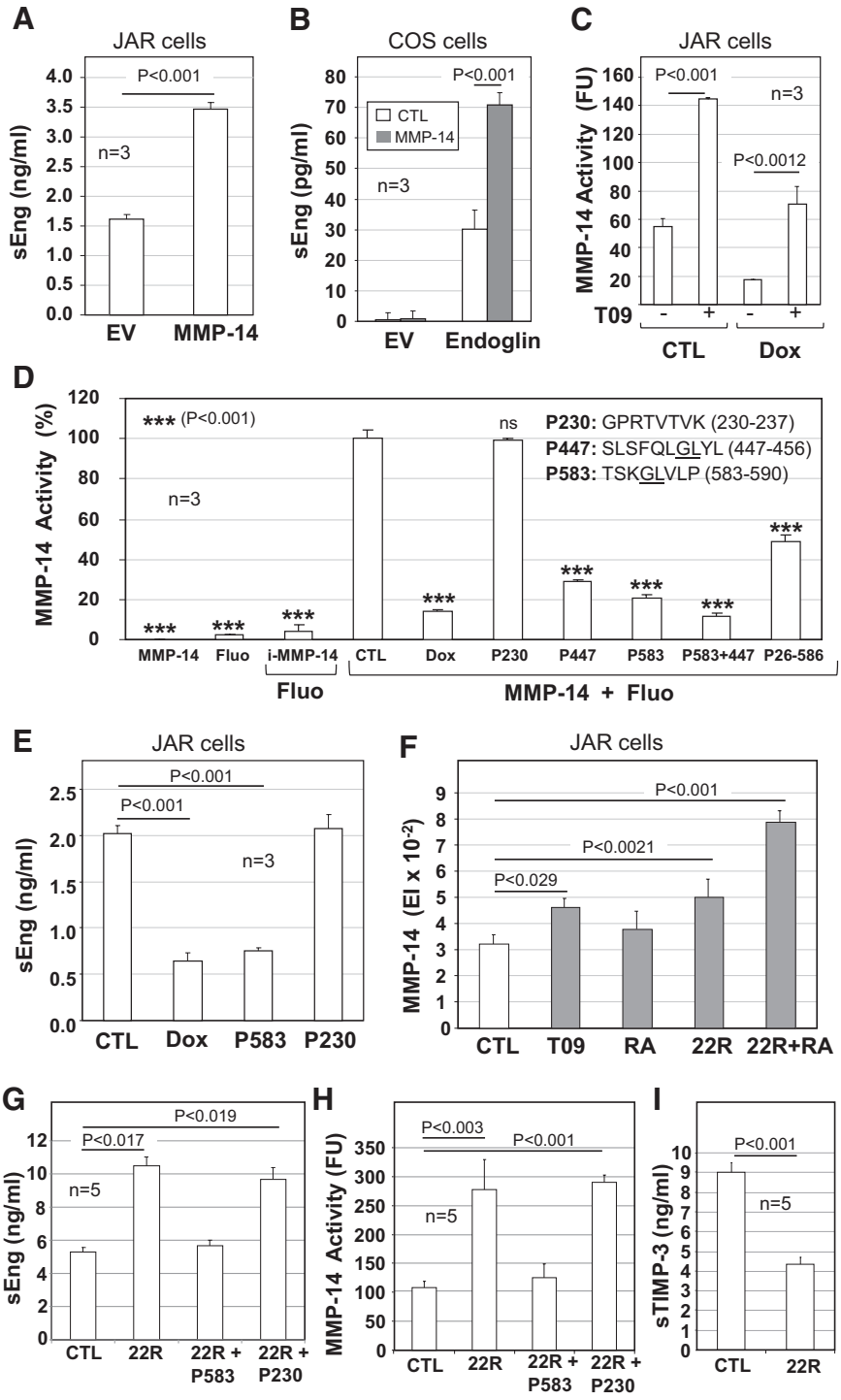

Figure 4. Involvement of matrix metalloproteinase (MMP)-14 in soluble endoglin (sEng) release. **A**, JAR cells were transiently transfected with an expression vector encoding MMP-14 or an empty vector (EV), and sEng in the media was measured by ELISA. **B**, COS cells, which do not express endoglin, were transiently cotransfected with an expression vector encoding endoglin or an empty vector either in the presence or in the absence of an expression vector encoding MMP-14. Levels of sEng in the culture media were measured by ELISA. Comparisons between groups were performed by *t* test. **C**, JAR cells were treated in the presence or in the absence of T09 or the MMP inhibitor doxycycline (Dox) for 24 hours as indicated. Then, the MMP-14 fluorogenic substrate Mca-PLGL-Dpa-AR-NH_2 (Fluo) was added to the culture, and fluorescence units (FU) were measured. Comparisons between groups were performed by *t* test. **D**, Effect of endoglin peptides on the MMP-14 activity. In a cell-free system, recombinant human MMP-14 was activated with aminophenylmercuric acetate, and the fluorogenic substrate Fluo was added in the presence or absence of endoglin peptides (P230, P447, or P583) or a recombinant version of the extracellular domain of human endoglin (Glu26-Gly586, P26–586). Negative controls, including MMP-14, the fluorogenic substrate (Fluo), and inactive MMP-14 (iMMP-14), are indicated. After incubation for 1 hour at 37°C, stop solution was added and fluorescence was measured. Every treatment was compared with the control (CTL; ***$P<0.001$; comparisons by 1-way ANOVA followed by *t* test). **E**, Effect of endoglin peptides on sEng release. JAR cells were cultured for 24 hours in the presence of endoglin peptides P583 (target of MMP-14 activity) and P230 (negative control) or doxycycline as indicated. Culture media

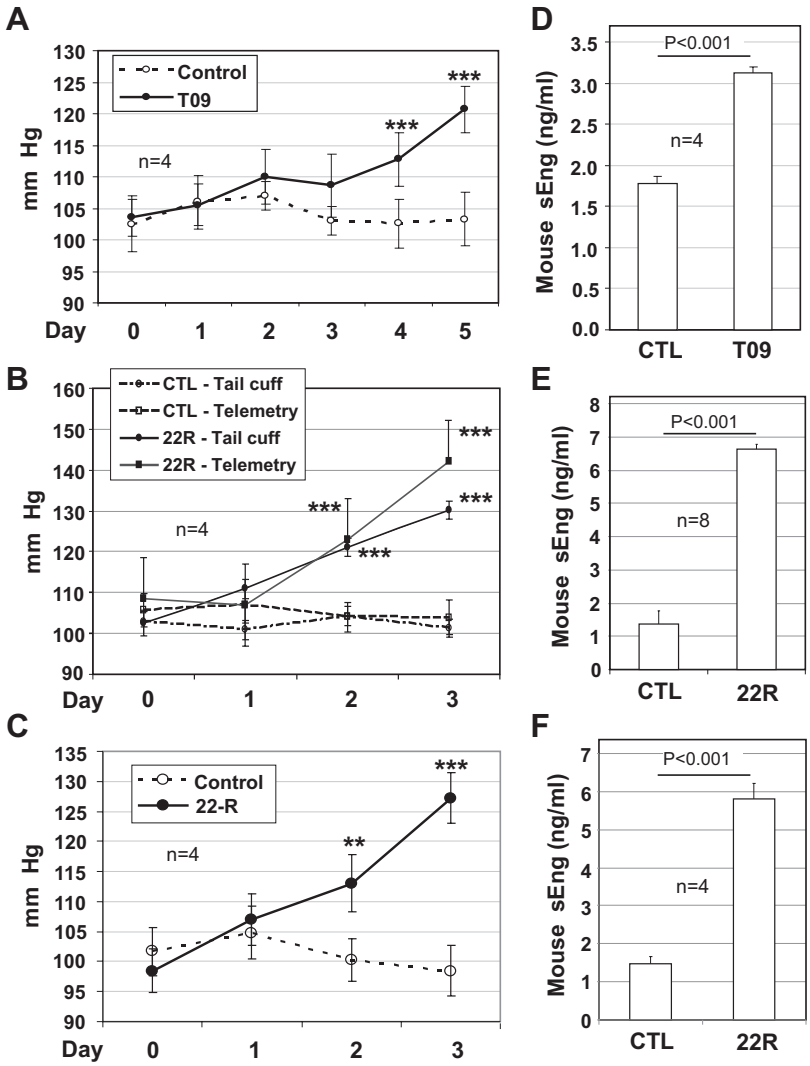

Figure 5. Effect of liver X receptor (LXR) ligands on arterial pressure. Male mice were intraperitoneally injected daily with T0901317 (**A** and **D**) or vehicle (Control). Male (**B** and **E**) or pregnant female (**C** and **F**) mice were intravenously injected daily with 22(R)-hydroxycholesterol (22-R; **B**, **C**, **E**, and **F**) or vehicle. During treatment, the systolic arterial pressure was measured daily with a tail cuff sphygmomanometer (**A–C**) or by telemetry (**B**). On the last day of treatment, tail cuff measurements were confirmed with an intracarotid blood pressure transducer in pregnant females (**C**). On the last day of treatment, mice were euthanized, serum samples were collected, and the soluble endoglin (sEng) levels were determined by ELISA (**D–F**). The number (n) of animals used in each treatment is indicated. Analysis was done by 2-way ANOVA with 1 fixed factor (treatment) and repeated measures (time); for every time point, the *t* test was made (control vs treatment) in **A** through **C**. In **A**, from day 4 of treatment, there is a statistical difference between T09 and control (CTL) group (*t* test, confidence level=0.005). In **B**, from day 2, there is a statistical difference between the 22-R and control groups in tail cuff and telemetry measurements, respectively (*t* test, confidence level=0.005). In **C**, there is a statistical difference from day 2 between the 22-R and control groups (*t* test, confidence level=0.001 in day 2 and 0.005 in day 3). ***$P<0.001$; **$P<0.005$. In **D** through **F**, differences were assessed by *t* test.

male mice were treated with the LXR synthetic agonist T09 or the physiological LXR ligand 22-R for 5 days. Figure 5A and 5B shows that the systolic arterial pressure, measured by tail cuff and telemetry, was steadily increased during treatment with both ligands. Similarly, pregnant female mice treated with 22-R displayed a marked increase in systolic arterial pressure, as evidenced by tail cuff and direct intracarotid measurements (Figure 5C). Of note, parallel measurements of diastolic and mean arterial pressure in mice treated with 22-R (Figure 5B) showed a response similar to systolic arterial pressure (Figure IV in the online-only Data Supplement). All mice treated with T09 or 22-R showed increased levels of sEng (Figure 5D–5F). In addition, mice treated with 22-R presented proteinuria (Figure V in the online-only Data Supplement), a symptom associated with preeclampsia.

The putative pathogenic role in vivo of MMP-14 and its product sEng in the hypertensive response was assessed by studying 2 different mouse models in which MMP-14 or sEng is overexpressed. Transgenic mice with a conditionally regulated MMP-14 allele were generated so that MMP-14 gene expression could be regulated by dietary doxycycline administration (Figure 6A and 6B and Figure VI in the online-only Data Supplement). In the presence of doxycycline, transcription of MMP-14 is blocked, whereas in the absence of doxycycline, MMP-14 expression is stimulated. Interestingly, upregulation of MMP-14 in the knock-in mice after 4 months was associated with an increase in systolic arterial pressure (Figure 6C) and plasma levels of sEng (Figure 6D). Of note, 2 months after upregulation of MMP-14, the arterial pressure was unaffected, although a small increase in plasma sEng

Figure 4 (Continued). were collected, and sEng levels were analyzed by ELISA. Comparisons were performed by 1-way ANOVA followed by *t* test. **F**, Effect of liver X receptor (LXR) ligands on MMP-14 expression. JAR cells were incubated with T09, retinoic acid (RA), 22(R)-hydroxycholesterol (22-R), or vehicle (CTL) for 24 hours as indicated. Then, cell surface MMP-14 was analyzed by immunofluorescence flow cytometry with an anti–MMP-14 monoclonal antibody (Figure III in the online-only Data Supplement), and the expression index (EI) of membrane-bound MMP-14 was represented (n=3 in each group; comparisons were performed by 1-way ANOVA followed by *t* test). **G** through **I**, A pool of human placental explants from 5 different donors was incubated with 22-R, vehicle, or endoglin peptides P583 and P230 for 24 hours as indicated. Culture media were collected, and sEng (**G**) and TIMP-3 (**I**) levels were analyzed by ELISA. Comparisons were performed by 1-way ANOVA followed by *t* test. **H**, Cultured explants were incubated with the Fluo, and fluorescence units were measured. Comparisons were made by *t* test.

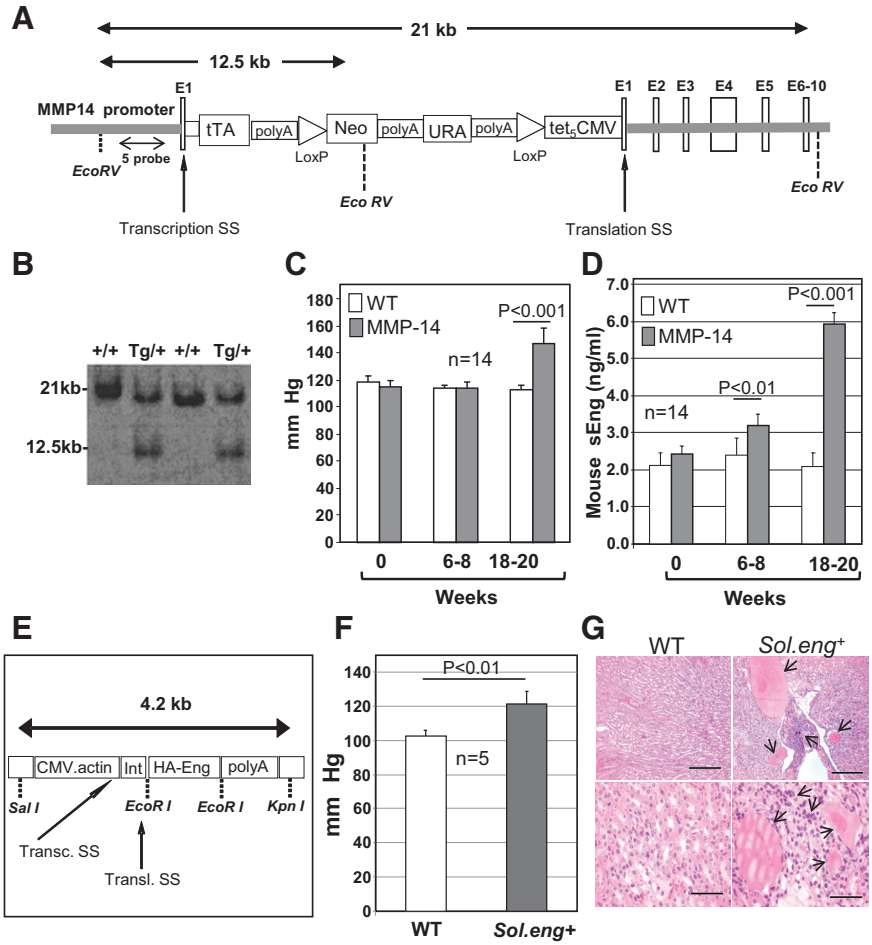

Figure 6. Effect of matrix metalloproteinase (MMP)-14 and soluble endoglin (sEng) overexpression on arterial pressure. **A** through **D**, MMP-14 overexpression in mice. **A**, Schematic representation of the conditionally regulated MMP-14 allele. The regulatory tTA-Neo-Ura-tet$_{05}$CMV-cassette was inserted immediately upstream of the translational initiation site of MMP-14. Transgenic animals were screened by *Eco*RV digestion of genomic DNA, followed by hybridization with a radiolabeled 5′ probe. Transcription and translation start sites (SS) are indicated. **B**, Southern blot analysis of heterozygous and wild-type (WT) mice. Probing of *Eco*RV-digested DNA revealed 21- and 12.5-kb fragments for WT and targeted (Tg) alleles. **C**, The systolic arterial pressure was measured, at the indicated times after induction of MMP-14, with a tail cuff sphygmomanometer in WT and MMP-14 knock-in inducible mice. In parallel, serum samples were collected from the tail at the times indicated, and the sEng levels were determined by ELISA (**D**). The number (n=14) of animals used in each measurement is indicated. Differences between groups were assessed by 2-way ANOVA followed by *t* test. **E** and **F**, sEng overexpression in mice. **E**, Schematic representation of the DNA construct used to generate transgenic mice expressing sEng. A 4.2-kb *Sal*I/*Kpn*I fragment, containing a cytomegalovirus enhancer and an actin promoter (CMV.actin), a β-globin intron (Int), the human endoglin cDNA (HA-Eng; inserted into *Eco*RI), and a β-globin polyadenylation site (polyA), was microinjected in the pronuclei of fertilized oocytes. **F**, Systolic arterial pressure was measured by telemetry in 3-month-old WT and *Sol.eng*$^+$ transgenic mice. Differences between groups were assessed by 2-way ANOVA followed by *t* test. **G**, Representative images of renal medullary area from *Sol.eng*$^+$ and WT mice showing the presence of dilated tubules filled with hyaline casts (arrows) and infiltrated cells in kidneys of *Sol.eng*$^+$ mice. Bars=480 μm in top images and 100 μm in bottom images.

could be measured, suggesting that the increased arterial pressure is not a consequence of the tetracycline removal per se but is dependent on the increased MMP activity. Similarly, transgenic mice overexpressing human sEng (*Sol.eng*$^+$) and with high plasma levels of human sEng (2050±618 ng/mL; undetectable in WT mice) showed increased levels of systolic arterial pressure compared with WT animals (Figure 6E and 6F). In addition, systolic, mean, and diastolic arterial pressures were higher in *Sol.eng*$^+$ mice (137±7, 119±6, and 102±6 mm Hg, respectively; n=5) than in WT male mice (106±6, 94±6, and 81±5 mm Hg, respectively; $P<0.05$ versus *Sol.eng*$^+$). Nonpregnant *Sol.eng*$^+$ females showed a systolic arterial pressure (tail cuff method; 121.7±4.1 mm Hg; n=7) significantly higher than that of nonpregnant WT females (108.6±0.4 mm Hg; n=7; $P<0.05$). When pregnant, *Sol.eng*$^+$ females showed a slight increase in arterial pressure (123.4±2.7 mm Hg), whereas there was a slight decrease in arterial pressure (106.4±2.8 mm Hg) in pregnant WT animals. Furthermore, when *Sol-eng*$^+$ females were crossed with CD1xC57BL/6J hybrid males, there were significant changes in litter size and pup weight. The average weight of pups from *Sol-eng*$^+$ mothers (5 litters, 35 pups) was 0.90±0.03 g compared with 1.21±0.003 g in WT mothers ($P<0.001$; 6 litters, 53 pups). Moreover, the number of pups per litter was significantly lower in *Sol.eng*$^+$ mothers (6.8±0.6) than in WT mothers (8.7±0.9; $P<0.01$). When *Sol.eng*$^+$ male mice were crossed with female CD1xC57BL/6J hybrids (36 litters, 234 pups), the number of pups per litter was similar to that of

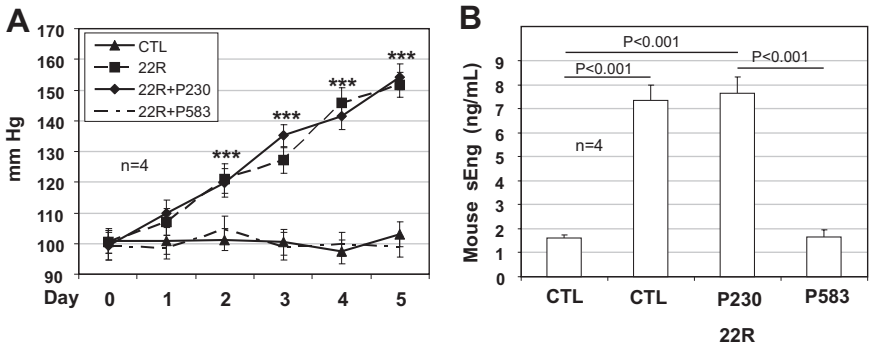

Figure 7. Effect of endoglin peptides on the increased arterial pressure induced by oxysterols. **A**, Mice were intravenously injected daily with vehicle (CTL) or 22(R)-hydroxycholesterol (22-R) in the absence or presence of the endoglin peptides P230 or P583 as indicated. During the treatment, systolic arterial pressure was measured daily with a tail cuff sphygmomanometer (**A**). On the last day of treatment, mice were euthanized, serum samples were collected, and the soluble endoglin (sEng) levels were determined by ELISA (**B**). The number (n=4) of animals used in each treatment is indicated. Analysis was done by 2-way ANOVA with 1 fixed factor (treatment) and repeated measures (time); for every time comparisons, *t* test was made (22-R–treated samples vs untreated group; there is a statistical difference from day 2 between the 22-R and control groups; *t* test, confidence level=0.005). In 22-R/P583–treated samples vs the 22-R/P230–treated group, there is a statistical difference from day 2 (confidence level=0.005).

hybrid/hybrid (24 litters, 153 pups) crosses (6.36±0.51 in WT/WT and 6.5±0.27 in *Sol.eng*$^+$/WT). Although *Sol.eng*$^+$ transgenic mice showed mainly normal kidney histology, dilated tubules containing hyaline casts in the medullary area and focal areas of inflammatory infiltrates were observed (Figure 6G). These findings are probably associated with increased protein content in the tubular fluid. Thus, the excess of sEng gives a phenotype that resembles preeclampsia (hypertension, small pup size, proteinuria, and renal damage). These results suggest that both MMP-14 and circulating sEng may contribute to the hypertensive phenotype.

Endoglin Peptide Can Inhibit Oxysterol-Induced Endoglin Shedding and Systolic Arterial Pressure

Because the endoglin peptide P583 can interfere with the MMP-14 activity and the proteolytic processing of membrane-bound endoglin in vitro, we assessed its effects in vivo. Intravenous injection of the oxysterol 22-R led to a marked increase in systolic arterial pressure that was clearly inhibited by coadministration of P583 (Figure 7A). Of note, P583 also reduced the levels of sEng (Figure 7B), suggesting that the oxysterol-dependent hypertensive effect of this animal model is mediated by sEng. In contrast, coinjection of 22-R and the endoglin peptide P230 did not affect the systolic arterial pressure or the sEng levels.

Discussion

Preeclampsia is one of the most severe complications of pregnancy. It is responsible for the highest rates of morbidity and mortality for both pregnant women and neonates. Even though over the last 20 years a great deal of evidence has accumulated on the pathophysiology of preeclampsia, the exact underlying mechanism remains to be elucidated. It is commonly accepted that its pathogenesis is associated with a hypoxic placenta. Placental hypoxia is responsible for the maternal vascular dysfunction via the increased placental release of antiangiogenic factors such as sFlt-1 and sEng. These soluble receptors bind vascular endothelial growth factor, placental growth factor, and members of the transforming growth factor-β superfamily in the maternal circulation, contributing to endothelial dysfunction in the maternal tissues.[26] Normal pregnancy is also characterized by systemic inflammation, oxidative stress, and alterations in levels of angiogenic factors and vascular reactivity. Both the placenta and maternal vasculatures are major sources of ROS and reactive nitrogen species that can produce powerful prooxidants that covalently modify proteins and alter vascular function in preeclampsia. Recent studies have shown that reduced uteroplacental perfusion causing placental ischemia results in an increase in serum sFlt-1 and sEng levels, thus firmly linking placental ischemia to upregulation of these antiangiogenic factors.[27] However, these studies have not elucidated the mechanism underlying the ischemia-induced upregulation of these antiangiogenic factors. Here, we have focused on the sEng shedding mechanism, dissecting the pathway involved (Figure 8). Our data suggest that increased levels of sEng are a consequence of hypoxia, as demonstrated with experiments in JAR cells and stable cell transfectants expressing human endoglin, as well as by hypoxia-inducible factor-1α silencing experiments (Figure 1). The triggering of the hypoxia pathway involves the generation of ROS (Figure 1E and 1F). This finding fits well with the increased levels and the postulated pathogenic role of ROS in preeclampsia.[5] Because cholesterol is a natural target of the ROS reactivity yielding oxysterols, we then assessed the possible involvement of oxysterols and their specific LXR receptor in the generation of sEng. We found that oxysterols enhance sEng levels acting at 3 different levels. Thus, oxysterols increase cell surface endoglin in agreement with a previous report[24]; increase the cell surface expression of MMP-14, a membrane-bound protease that can cleave cell surface endoglin[33]; and inhibit the expression of TIMP-3, an inhibitor of MMP-14. The net oxysterol-dependent upregulation of sEng is specifically dependent on the LXR pathway, as demonstrated in *LXR*$\alpha,\beta^{-/-}$ murine embryonic fibroblasts, suggesting that LXRs play a pivotal role in the sEng shedding (Figure 2C). Because normal pregnancy is associated with an enhanced oxidation of LDL particles and in preeclamptic pregnancies there is evidence of abnormally enhanced production of lipid

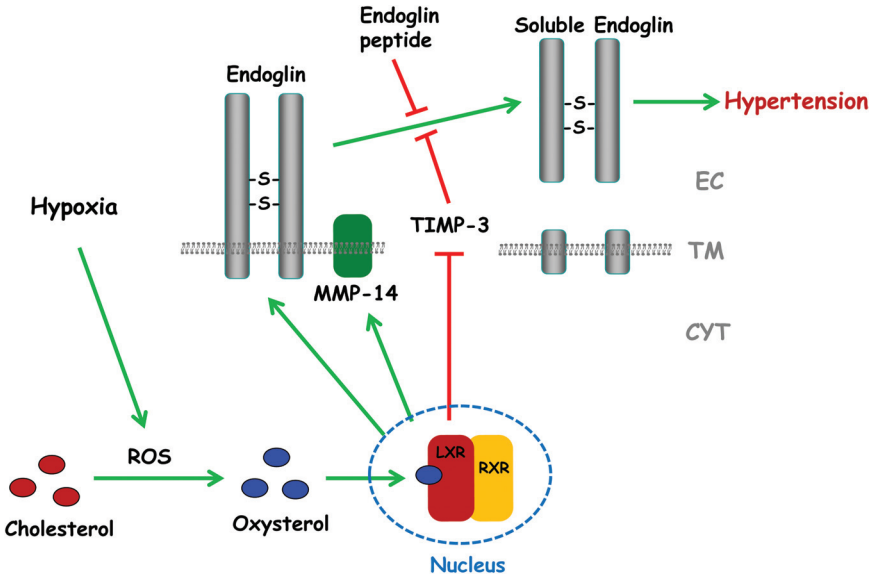

Figure 8. Hypothetical model of the generation and role of soluble endoglin (sEng) in vascular homeostasis. Hypoxia induces reactive oxygen species (ROS), which in turn convert cholesterol into oxysterol species. Oxysterols specifically bind to nuclear liver X receptor (LXR)/retinoic X receptor (RXR) dimeric receptors, leading to increased matrix metalloproteinase-14 (MMP-14) levels and decreased levels of the MMP-14 inhibitor tissue inhibitor of metalloproteinase-3 (TIMP-3). As a result, there is increased MMP-14 activity that proteolytically cleaves the juxtamembrane region of membrane-bound endoglin and generates a soluble form (sEng). Increased levels of sEng lead to increased systemic arterial pressure in mice. Treatment with an endoglin peptide that is a substrate of MMP-14 counteracts the hypertension induced by oxysterols in vivo. The extracellular (EC), transmembrane (TM), and cytoplasmic (CYT) domains, as well as the disulfide bonds (-S-) of endoglin are indicated.

peroxides in maternal blood,[41] it can be speculated that an increased internalization of oxysterols in trophoblasts might activate LXR and increase membrane and sEng levels. In this regard, human trophoblasts have been shown to express very high levels of surface endoglin.[30] Of note, several lines of evidence support the involvement of the LXR pathway in trophoblast biology. Thus, oxysterols inhibit differentiation and fusion of term primary trophoblasts via LXR.[12] In addition, lipids from oxidized low-density lipoprotein and other LXR agonists modulate human trophoblast invasion by activating LXRs.[21,42] Because endoglin expression regulates trophoblast differentiation and invasion of extravillous trophoblasts,[32,43] it will be interesting to dissect the specific contribution of the LXR-induced soluble form of endoglin in these processes.

Although the activation of the LXR pathway leads to an enhanced transcription and, in turn, increased surface expression of endoglin,[24] our data indicate that the oxysterol-induced concentrations of sEng are due not only to the higher amounts of surface endoglin but also to the increased activity of MMP-14. Supporting this view, stable cell transfectants of endoglin, which lack the LXR-responsive elements in the endoglin promoter,[24] are also able to induce shedding of sEng in response to the activation of LXR (Figure 2D). One target gene of LXR is TIMP-3 (Figure 3), a member of a family of 4 secreted proteins (TIMP-1–TIMP-4) that are endogenous inhibitors of MMPs. Because TIMP-3 is an inhibitor of MMP-14, the downregulation of TIMP-3, triggered by LXR, may lead to activation of MMP-14. Our data not only support this view but also provide evidence for an upregulation of the MMP-14 levels at the cell surface on LXR activation (Figures 3 and 4), suggesting that gene expression of TIMP-3 and gene expression of MMP-14 are timely coordinated to regulate sEng shedding. Interestingly, the in vitro results were confirmed by experiments in vivo. Thus, administration of T09 or the oxysterol 22-R to mice led to a marked increase in the levels of sEng (Figure 5). Compatible with the involvement of MMP-14 in this process, we found that MMP-14–overexpressing mice also showed increased levels of sEng compared with WT mice (Figure 6D). On the basis of the capacity of the endoglin peptide P583, containing the GL cleavage motif, to interfere with the MMP-14 activity and the proteolytic processing of membrane-bound endoglin in vitro, we studied the effects of this peptide in vivo. Intravenous coinjection of P583 with the oxysterol 22-R led to an abolishment of the LXR-induced shedding of sEng, suggesting that this peptide may be a useful therapeutic drug.

The in vivo experiments showed that administration of the LXR agonist T09 or the oxysterol 22-R induced not only increased levels of sEng but also a marked increase in arterial pressure. This is in agreement with the association between a common polymorphism in the LXR-β gene and preeclampsia,[44] the increase in sEng in preeclampsia, and the reported pathogenic role of sEng in hypertension. Further support for this hypothesis was obtained from transgenic mice overexpressing human sEng that displayed a clear increase in arterial pressure associated with high levels of circulating sEng (Figure 6F). These data underline the importance of the oxysterol/LXR pathway in modifying arterial pressure.

Treatment of hypertension is especially needed in preeclampsia owing to the absence of effective therapies. However, some hope may arise from the in vivo studies using the endoglin peptide P583. Indeed, intravenous coinjection of P583 with the oxysterol 22-R led to the inhibition of the

LXR-induced systolic arterial pressure. Because the sequence of P583 corresponds to TSKGLVLP (amino acids 583–590), which includes the MMP-14 cleavage site GL, the likely mechanism of action for P583 is the competition with membrane endoglin for MMP-14 cleavage. An obvious potential application of these studies is the therapeutic use of this kind of peptide in preeclamptic women to counteract the pathogenic effect of the elevated circulating sEng levels in these patients. Further studies are needed to confirm the counterhypertensive effect of this peptide in experimental models of preeclampsia and in clinical trials.

Finally, in addition to preeclampsia, increased levels of circulating sEng in serum, plasma, and other fluids in patients suffering from different diseases, including cancer and pathologies associated with endothelial dysfunction such as hypertension and diabetes mellitus, have been reported.[29,45–47] Because elevated sEng levels are associated with poor prognosis in patients with metastatic solid tumors and with higher target-organ damage in hypertensive and diabetic patients,[46] these studies may also help us understand the function of sEng in those pathological settings.

Acknowledgments

We thank Annette Düwell for excellent technical assistance, Lucía Martin for care and genotyping of transgenic mice, Dr Alicia Prieto for mass spectrometry analysis, Dr Manuel A. Sanchez-Martin (Genetically Modified Organisms Unit, University of Salamanca) for generation of transgenic mice, Professor Miguel Arevalo (Department of Anatomy and Histology, University of Salamanca) for $sEng^{+}$ kidney histology, Professor Juan L. Lanchares (Department of Obstetrics and Gynecology, University Hospital, Salamanca) and Rosario Gonzalez (delivery room supervisor) for providing us with placentas, Dr David Mangelsdorf for the $LXR^{-/-}$ mice housed in Dr Castrillo's laboratory, and Dr Laura Barrios (Centro Tecnico de Informatica, CTI-CSIC, Madrid) for statistical analysis of the data.

Sources of Funding

This work was supported by grants from the Ministerio de Ciencia e Innovación of Spain (SAF2010-61827 to Dr Bernabeu, SAF2011-29244 to Dr Castrillo, and SAF2010-15881 to Dr Lopez-Novoa), Genoma España (MEICA; Dr Bernabeu), Instituto Reina Sofía de Investigación Nefrológica (FRIAT; Dr Lopez-Novoa), Junta de Castilla and Leon (Excellence Group Grant GR-100 to Dr Lopez-Novoa), Centro de Investigación Biomédica en Red de Enfermedades Raras (CIBERER; Dr Bernabeu), and Red de Investigación Cooperativa en Enfermedades Renales (REDINREN; Dr Lopez-Novoa). CIBERER and REDINREN are initiatives of the Instituto de Salud Carlos III of Spain supported by European Regional Development Funds (FEDER). The cardiovascular phenotyping unit, including the telemetry equipment, has been acquired with the support of FEDER. Dr Llano is recipient of a Ramón y Cajal Research contract.

Disclosures

Drs Valbuena-Diez, Blanco, Lopez-Novoa, and Bernabeu and C. Langa are scientific authors of a patent application filed in the Spanish Patent Office and owned by CSIC, USAL, and CIBERER on the use of an endoglin peptide to prevent sEng release and its effects. The other authors report no conflicts.

References

1. Sibai B, Dekker G, Kupferminc M. Pre-eclampsia. *Lancet*. 2005;365:785–799.
2. Young BC, Levine RJ, Karumanchi SA. Pathogenesis of preeclampsia. *Annu Rev Pathol*. 2010;5:173–192.
3. Khong TY, De Wolf F, Robertson WB, Brosens I. Inadequate maternal vascular response to placentation in pregnancies complicated by pre-eclampsia and by small-for-gestational age infants. *Br J Obstet Gynaecol*. 1986;93:1049–1059.
4. Soleymanlou N, Jurisica I, Nevo O, Ietta F, Zhang X, Zamudio S, Post M, Caniggia I. Molecular evidence of placental hypoxia in preeclampsia. *J Clin Endocrinol Metab*. 2005;90:4299–42308.
5. Al-Gubory KH, Fowler PA, Garrel C. The roles of cellular reactive oxygen species, oxidative stress and antioxidants in pregnancy outcomes. *Int J Biochem Cell Biol*. 2010;42:1634–1650.
6. Duranteau J, Chandel NS, Kulisz A, Shao Z, Schumacker PT. Intracellular signaling by reactive oxygen species during hypoxia in cardiomyocytes. *J Biol Chem*. 1998;273:11619–11624.
7. Nakagawara A, DeSantis NM, Nogueira N, Nathan CF. Lymphokines enhance the capacity of human monocytes to secret reactive oxygen intermediates. *J Clin Invest*. 1982;70:1042–1048.
8. Janowski BA, Willy PJ, Devi TR, Falck JR, Mangelsdorf DJ. An oxysterol signalling pathway mediated by the nuclear receptor LXR alpha. *Nature*. 1996;383:728–731.
9. Lehmann JM, Kliewer SA, Moore LB, Smith-Oliver TA, Oliver BB, Su JL, Sundseth SS, Winegar DA, Blanchard DE, Spencer TA, Willson TM. Activation of the nuclear receptor LXR by oxysterols defines a new hormone response pathway. *J Biol Chem*. 1997;272:3137–3140.
10. Schroepfer GJ Jr. Oxysterols: modulators of cholesterol metabolism and other processes. *Physiol Rev*. 2000;80:361–554.
11. Steck TL, Lange Y. Cell cholesterol homeostasis: mediation by active cholesterol. *Trends Cell Biol*. 2010;20:680–687.
12. Aye IL, Waddell BJ, Mark PJ, Keelan JA. Oxysterols inhibit differentiation and fusion of term primary trophoblasts by activating liver X receptors. *Placenta*. 2011;32:183–191.
13. Janowski BA, Grogan MJ, Jones SA, Wisely GB, Kliewer SA, Corey EJ, Mangelsdorf DJ. Structural requirements of ligands for the oxysterol liver X receptors LXRalpha and LXRbeta. *Proc Natl Acad Sci U S A*. 1999;96:266–271.
14. Kalaany NY, Mangelsdorf DJ. LXRS and FXR: the yin and yang of cholesterol and fat metabolism. *Annu Rev Physiol*. 2006;68:159–191.
15. El-Hajjaji FZ, Oumeddour A, Pommier AJ, Ouvrier A, Viennois E, Dufour J, Caira F, Drevet JR, Volle DH, Baron S, Saez F, Lobaccaro JM. Liver X receptors, lipids and their reproductive secrets in the male. *Biochim Biophys Acta*. 2011;1812:974–981.
16. Calkin AC, Tontonoz P. Liver X receptor signaling pathways and atherosclerosis. *Arterioscler Thromb Vasc Biol*. 2010;30:1513–1518.
17. A-González N, Castrillo A. Liver X receptors as regulators of macrophage inflammatory and metabolic pathways. *Biochim Biophys Acta*. 2011;1812:982–994.
18. Schultz JR, Tu H, Luk A, Repa JJ, Medina JC, Li L, Schwendner S, Wang S, Thoolen M, Mangelsdorf DJ, Lustig KD, Shan B. Role of LXRs in control of lipogenesis. *Genes Dev*. 2000;14:2831–2838.
19. Repa JJ, Mangelsdorf DJ. The role of orphan nuclear receptors in the regulation of cholesterol homeostasis. *Annu Rev Cell Dev Biol*. 2000;16:459–481.
20. Baranowski M. Biological role of liver X receptors. *J Physiol Pharmacol*. 2008;59:31–55.
21. Pavan L, Hermouet A, Tsatsaris V, Thérond P, Sawamura T, Evain-Brion D, Fournier T. Lipids from oxidized low-density lipoprotein modulate human trophoblast invasion: involvement of nuclear liver X receptors. *Endocrinology*. 2004;145:4583–4591.
22. Marceau G, Volle DH, Gallot D, Mangelsdorf DJ, Sapin V, Lobaccaro JM. Placental expression of the nuclear receptors for oxysterols LXRalpha and LXRbeta during mouse and human development. *Anat Rec A Discov Mol Cell Evol Biol*. 2005;283:175–181.
23. Weedon-Fekjaer MS, Duttaroy AK, Nebb HI. Liver X receptors mediate inhibition of hCG secretion in a human placental trophoblast cell line. *Placenta*. 2005;26:721–728.
24. Henry-Berger J, Mouzat K, Baron S, Bernabeu C, Marceau G, Saru JP, Sapin V, Lobaccaro JM, Caira F. Endoglin (CD105) expression is regulated by the liver X receptor alpha (NR1H3) in human trophoblast cell line JAR. *Biol Reprod*. 2008;78:968–975.
25. Venkatesha S, Toporsian M, Lam C, Hanai J, Mammoto T, Kim YM, Bdolah Y, Lim KH, Yuan HT, Libermann TA, Stillman IE, Roberts D, D'Amore PA, Epstein FH, Sellke FW, Romero R, Sukhatme VP, Letarte M, Karumanchi SA. Soluble endoglin contributes to the pathogenesis of preeclampsia. *Nat Med*. 2006;12:642–649.

26. Powe CE, Levine RJ, Karumanchi SA. Preeclampsia, a disease of the maternal endothelium: the role of antiangiogenic factors and implications for later cardiovascular disease. *Circulation*. 2011;123:2856–2869.
27. Foidart JM, Schaaps JP, Chantraine F, Munaut C, Lorquet S. Dysregulation of anti-angiogenic agents (sFlt-1, PLGF, and sEndoglin) in preeclampsia: a step forward but not the definitive answer. *J Reprod Immunol*. 2009;82:106–111.
28. Aoki Y, Yamamoto T, Fumihisa C, Nakamura A, Asanuma A, Suzuki M. Effect on the production of soluble endoglin from human choriocarcinoma cells by preeclampsia sera. *Am J Reprod Immunol*. 2012;67:413–420.
29. López-Novoa JM, Bernabeu C. The physiological role of endoglin in the cardiovascular system. *Am J Physiol Heart Circ Physiol*. 2010;299:H959–H974.
30. Gougos A, St Jacques S, Greaves A, O'Connell PJ, d'Apice AJ, Bühring HJ, Bernabeu C, van Mourik JA, Letarte M. Identification of distinct epitopes of endoglin, an RGD-containing glycoprotein of endothelial cells, leukemic cells, and syncytiotrophoblasts. *Int Immunol*. 1992;4:83–92.
31. Letamendía A, Lastres P, Almendro N, Raab U, Bühring HJ, Kumar S, Bernabéu C. Endoglin, a component of the TGF-beta receptor system, is a differentiation marker of human choriocarcinoma cells. *Int J Cancer*. 1998;76:541–546.
32. Caniggia I, Taylor CV, Ritchie JW, Lye SJ, Letarte M. Endoglin regulates trophoblast differentiation along the invasive pathway in human placental villous explants. *Endocrinology*. 1997;138:4977–4988.
33. Hawinkels LJ, Kuiper P, Wiercinska E, Verspaget HW, Liu Z, Pardali E, Sier CF, ten Dijke P. Matrix metalloproteinase-14 (MT1-MMP)-mediated endoglin shedding inhibits tumor angiogenesis. *Cancer Res*. 2010;70:4141–4150.
34. Castonguay R, Werner ED, Matthews RG, Presman E, Mulivor AW, Solban N, Sako D, Pearsall RS, Underwood KW, Seehra J, Kumar R, Grinberg AV. Soluble endoglin specifically binds bone morphogenetic proteins 9 and 10 via its orphan domain, inhibits blood vessel formation, and suppresses tumor growth. *J Biol Chem*. 2011;286:30034–30046.
35. Letamendía A, Lastres P, Botella LM, Raab U, Langa C, Velasco B, Attisano L, Bernabeu C. Role of endoglin in cellular responses to transforming growth factor-beta: a comparative study with betaglycan. *J Biol Chem*. 1998;273:33011–33019.
36. Bellón T, T, Corbí A, Lastres P, Calés C, Cebrián M, Vera S, Cheifetz S, Massague J, Letarte M, Bernabéu C. Identification and expression of two forms of the human transforming growth factor-beta-binding protein endoglin with distinct cytoplasmic regions. *Eur J Immunol*. 1993;23:2340–2345.
37. Guerrero-Esteo M, Sanchez-Elsner T, Letamendia A, Bernabeu C. Extracellular and cytoplasmic domains of endoglin interact with the transforming growth factor-beta receptors I and II. *J Biol Chem*. 2002;277:29197–29209.
38. Bligh EG, Dyer WJ. A rapid method of total lipid extraction and purification. *Can J Biochem Physiol*. 1959;37:911–917.
39. Murphy RC, Johnson KM. Cholesterol, reactive oxygen species, and the formation of biologically active mediators. *J Biol Chem*. 2008;283:15521–15525.
40. Hoe HS, Cooper MJ, Burns MP, Lewis PA, van der Brug M, Chakraborty G, Cartagena CM, Pak DT, Cookson MR, Rebeck GW. The metalloprotease inhibitor TIMP-3 regulates amyloid precursor protein and apolipoprotein E receptor proteolysis. *J Neurosci*. 2007;27:10895–10905.
41. Walsh SW, Wang Y. Deficient glutathione peroxidase activity in preeclampsia is associated with increased placental production of thromboxane and lipid peroxides. *Am J Obstet Gynecol*. 1993;169:1456–1461.
42. Fournier T, Handschuh K, Tsatsaris V, Guibourdenche J, Evain-Brion D. Role of nuclear receptors and their ligands in human trophoblast invasion. *J Reprod Immunol*. 2008;77:161–170.
43. Mano Y, Kotani T, Shibata K, Matsumura H, Tsuda H, Sumigama S, Yamamoto E, Iwase A, Senga T, Kikkawa F. The loss of endoglin promotes the invasion of extravillous trophoblasts. *Endocrinology*. 2011;152:4386–4394.
44. Mouzat K, Mercier E, Polge A, Evrard A, Baron S, Balducchi JP, Brouillet JP, Lumbroso S, Gris JC. A common polymorphism in NR1H2 (LXRbeta) is associated with preeclampsia. *BMC Med Genet*. 2011;12:145.
45. Bernabeu C, Lopez-Novoa JM, Quintanilla M. The emerging role of TGF-beta superfamily coreceptors in cancer. *Biochim Biophys Acta*. 2009;1792:954–973.
46. Blazquez-Medela AM, Garcia-Ortiz L, Gomez-Marcos MA, Recio-Rodriguez JL, Sanchez-Rodriguez A, Lopez-Novoa JM, Martinez-Salgado C. Increased plasma soluble endoglin levels as an indicator of cardiovascular alterations in hypertensive and diabetic patients. *BMC Med*. 2010;8:86.
47. Fonsatti E, Nicolay HJ, Altomonte M, Covre A, Maio M. Targeting cancer vasculature via endoglin/CD105: a novel antibody-based diagnostic and therapeutic strategy in solid tumours. *Cardiovasc Res*. 2010;86:12–19.

CLINICAL PERSPECTIVE

Preeclampsia is one of the most severe complications of pregnancy. Characterized by systemic hypertension, proteinuria, and edema in the third trimester of pregnancy, preeclampsia is responsible for the highest rates of morbidity and mortality for both pregnant women and neonates in the developed world. Treatment of hypertension in preeclampsia is especially needed because of the absence of effective therapies except for the delivery of the baby and placenta. Hypoxia in the placenta is considered a key event in the pathogenesis of preeclampsia, whereas soluble endoglin (sEng) is a prognostic marker and plays a pathogenic role. In this article, we report that the hypoxia-dependent cholesterol derivatives oxysterols, via the liver X receptors, are able to increase sEng levels in vitro and in vivo by a mechanism involving activation of matrix metalloproteinase-14. Interestingly, mice treated with oxysterols or liver X receptor agonists underwent an increase in plasmatic sEng levels and an augmentation of arterial pressure. In addition, administration of an endoglin fragment containing the matrix metalloproteinase-14 cleavage site prevented the oxysterol-dependent increase in arterial pressure and sEng levels in mice. These data reveal for the first time the involvement of the liver X receptor pathway in sEng release and its contribution to vascular homeostasis. They also suggest that administration of endoglin peptides in preeclamptic women might serve to counteract the pathogenic effect of the elevated circulating sEng. Further studies are needed to confirm the beneficial effect of these peptides in experimental models of preeclampsia and in clinical trials.

SUPPLEMENTAL MATERIAL

EXPANDED METHODS

Cell Culture

The human placental choriocarcinoma cell line JAR was cultured in RPMI-1640.[1] The stable transfectants of rat myoblasts L6E9[2] and mouse fibroblasts L929[3] expressing human endoglin were grown in Dulbecco's modified Eagle's medium (DMEM) containing 0.4 mg/mL of geneticin (Calbiochem, San Diego, CA, USA). Human umbilical vein endothelial cells (HUVEC) were cultured in EBM2 medium supplemented with EGM2 (Lonza, Walkersville, MD, USA). Mouse embryonic fibroblasts (MEFs) from wild type (WT) and LXR knock-out mice ($Lxr\alpha,\beta^{-/-}$) mice and monkey kidney COS-7 cells were grown in DMEM medium. All the media were supplemented with 10% heat-inactivated fetal calf serum (FCS), 2 mM L-glutamine and 100 U/mL penicillin-streptomycin. Cells were cultured in a 5% CO_2 atmosphere at 37ºC. For LXR activation studies, cells were incubated for 24 hours with 1-5µM of the LXR synthetic agonist, T0901317 (Calbiochem), 5µM 22(R)-hydroxycholesterol (22-R), 10µM 9-cis-Retinoic acid (RA), both from Sigma-Aldrich (L'Isle D'Abeau, France), as indicated. For metalloprotease inhibition assays, cells were incubated for 24 hours with 10µg/mL rhTIMP-1, rhTIMP-2 or rhTIMP-3 (R&D Systems, Minneapolis, MN, USA), 50µM doxycyclin (Sigma-Aldrich, L'Isle D'Abeau, France) or 15µM endoglin peptides (described below). For hypoxia treatments, JAR cells were incubated under hypoxic conditions with 1% O_2 using a Modular Incubator Chamber MIC-101 (Billups-Rothenberg Inc., CA) or in the presence of 100µM deferoxiamine mesylate salt (DFO; Sigma-Aldrich, L'Isle D'Abeau, France) for 24 hours.

Human placental explants

Fresh placental explants were collected in the delivery room of University Hospital, Salamanca, within 30 minutes of delivery from patients without complications. Several cotyledons were excised at random and rinsed extensively in sterile saline to remove blood. Decidua and large vessels were removed. After removing the sterile saline tissue was weighed and precisely 500 mg of tissue was collected and placed into each well of a six-well plate containing 2 mL of complete DMEM-F12 medium (Sigma-Aldrich, L'Isle D'Abeau, France) containing 10% FCS. Explants were incubated at 37ºC for 6 hours and then for 24 hours with 5μM 22-R, as indicated. For metalloprotease inhibition assays, cells were incubated for 24 hours with 15μM endoglin peptides. The experimental protocol was in accordance with the Declaration of Helsinki (2000) of the World Medical Association and also was in agreement with the guidelines of and approved by the Ethics Committee of the University Hospital of Salamanca (Spain), and complied with Spanish data protection law 15/1999 and its developed specifications (RD 1720/2007). Each patient included in the study signed an informed consent form to participate in the investigation after full explanation of the purpose and nature of all procedures used. To guarantee data confidentiality, all the electronic and paper copies of the protocol, signed informed consent documents and results of the tests were kept locked in a safe place, and only the study investigators had access to the data on the people who agreed to participate in the study.

Plasmids and cell transfections

Expression vector encoding HA-tagged human endoglin in pDisplay has been described (4). Expression vector encoding human MT1-MMP driven by CMV promoter in pCI-neo was kindly provided by Dr. Alicia Garcia-Arroyo (Centro Nacional de Investigaciones Cardiovasculares, Madrid, Spain). Cell transfections were carried out with SuperFect Reagent (Qiagen, Crawley, UK), according to the manufacturer's instructions.

Flow cytometry

Flow cytometry analyses were performed with an EPICS XL equipment (Beckman Coulter). For immunofluorescence flow cytometry studies, cells were incubated with the primary antibodies mouse monoclonal anti-endoglin P4A4, rabbit monoclonal antibody to MMP-14 (Abcam, Cambridge, UK; clone #EP1264Y) or with control monoclonal antibodies for 60 minutes at 4ºC. After 2 washes with PBS, Alexa 488 anti-mouse or Alexa 647 anti-rabbit antibody was added and incubation was carried out for an additional period of 60 min at 4ºC. Finally, cells were washed twice and their fluorescence was estimated. For ROS detection analyses, JAR cells were submitted to hypoxia/normoxia for 24 hours in the presence or absence of 1mM of Trolox (Calbiochem), a cell-permeable, water-soluble derivative of vitamin E with antioxidant properties. After 24 hours, media were removed and cells were incubated with 10μM 2´,7´-dichlorodihydrofluorescein diacetate (CM-H2DCFDA; Invitrogen, Carlsbad, CA) and maintained at 37ºC in the dark for 60 minutes. Then cells were washed twice with PBS and their fluorescence was estimated.

ELISA

Mouse blood samples were centrifuged shortly after collection, and stored at -70ºC until assay. Concentrations of human sEng in conditioned media or in plasma from human sEng transgenic mice were determined by Quantikine Human Endoglin/CD105 (R&D Systems, Minneapolis, MN). The sensitivity of this ELISA kit allows a minimum detectable dose of human endoglin ranged from 0.001 to 0.030 ng/mL. Mouse blood samples were centrifuged shortly after collection, and stored at -70ºC until assay. The plasma concentrations of mouse sEng were determined by a DuoSet Mouse Endoglin/CD105 (R&D Systems, Minneapolis, MN). The sensitivity of this ELISA kit allows a minimum detectable dose of mouse endoglin of 0.05 ng/mL. Concentrations of TIMP-3 in the conditioned media were determined using a TIMP-3 human ELISA kit (Abnova, Taiwan). The sensitivity of this ELISA kit allows a minimum detectable concentration of human TIMP-3 of 156 pg/mL. All immunoassays used

the quantitative sandwich enzyme immunoassay technique and measures were read in a Varioskan Flash spectral scanning multimode reader (Thermo Scientific). The concentrations were determined by interpolation from a standard curve as indicated by the manufacturer.

Lipid analysis and liposome preparation

Lipid extraction was carried out according to the method of Bligh and Dyer.[5] Briefly, adherent JAR cells were scraped and resuspended in PBS. Then, 0.8 volume parts of aqueous cell homogenates were vigorously mixed with 3 volume parts of 1:2 (v/v) chloroform /methanol mixture and the sample was kept for about 5-10 minutes at room temperature. Next, the sample was mixed with 1 volume part of 1:1 (v/v) chloroform/water, vortexed and centrifuged at high speed (3,000 rpm) for 15 minutes at room temperature yielding a two phase system. The lower chloroform phase, containing the lipids, was isolated and submitted to gas chromatography-mass spectrometry (GC-MS) analysis. Prior to GC-MS analysis, lipids were derivitized to trimethylsilyl (TMS) ethers using bis(trimethylsilyl)trifluoroacetamide (BSTFA). To this end, the sample was transferred to a GC vial and mixed with 25 µL BSTFA and 25 µL pyridine. The vial was capped tightly and heated at 60ºC for ~45 minutes. The sample was allowed to cool down to room temperature and then injected on the GC-MS equipment (Agilent 7890A, Agilent Technologies). As control markers for GC-MS, purified cholesterol and 22-R were used.

Liposomes containing L-α-phosphatidylcholine (Sigma) and 22-R were prepared at a molar ratio of 2:1, respectively. Lipids were dissolved in chloroform, mixed vigorously in a conical tube and vacuum desiccated. The remaining viscous residue was resuspended in sterile PBS (pH 7.4). When necessary, endoglin peptides were added to the mixture. The aqueous suspension was bath-sonicated for 1 hr prior to injection into mice.

Real time and semiquantitative RT-PCR analysis of mRNA levels

Total RNA was isolated from cells with the RNeasy kit (Qiagen) and reverse-transcribed using iScript cDNA Synthesis kit (Bio-Rad Laboratories, Hercules, CA). For quantitative analysis, the resultant cDNA was used as a template for real time PCR using the iQ SyBR-Green Supermix (Bio-Rad, Hercules, CA, USA). Primers used for human TIMP-3 were: 5′-AGCTTCCGAGAGTCTCTGTG-3′ (Forward) and 5′-CACCTCTCCACGAAGTTGC-3′ (Reverse). Primers used for human TIMP-2 were: 5′-CCAAGCAGGAGTTTCTCGAC-3′ (Forward) and 5′-TTTCCAGGAAGGGATGTCAG-3′ (Reverse). Primers used to amplify HIF-1α were: 5′- TGATGACCAGCAACTTGAGG -3′ (Forward) and 5′-TTGATTGAGTGCAGGGTCAG -3′ (Reverse). Amplicons were detected using an iQ5 real time detection system. Transcript levels were normalized to 18S levels. Triplicates of each experiment were performed.

For semiquantitative RT-PCR, cDNA was subjected to PCR amplification using the HotMaster Taq DNA Polymerase kit (5 Prime Inc., Gaithersburg, MD) with the same human TIMP-3 primers described above and, as a control, human glyceraldehyde-3-phosphate dehydrogenase (GAPDH) primers: 5′-AGCCACATCGCTCAGACAC- 3′ (Forward) and 5′ -GCCCAATACGACCAAATCC- 3′ (Reverse). PCR products were separated by agarose gel electrophoresis. Gels were documented in a Gel Doc XR System (Bio-Rad, Hercules, CA) and bands were quantified using the Quantity One software.

RNA interference experiments

The human small interfering ribonucleic acids (siRNA) for TIMP-3 and HIF-1α were obtained from Ambion Inc. (Austin, USA; ref.# AM16708A). Three different siRNA were used for HIF-1α (144736, 106499 and 3187) and TIMP-3 (s14146, s14148 and s14147) as well as scrambled siRNA as controls. JAR cells were transfected with 5 pmoles of specific siRNA or scrambled siRNA, using Lipofectamine 2000 (Invitrogen, Carlsbad, CA, USA). Quantitative analysis of HIF-1α and TIMP-3 transcripts is described above.

Monitoring metalloproteinase activity using a synthetic fluorogenic substrate

To activate the metalloproteinase activity, JAR cells or placental explants were cultured in a 96-well or 6-well microplate, respectively, in the presence or absence of 5µM T09, 5µM 22-R, 10µM RA or 50µM doxycyclin during 24 hours, as indicated. After 24 hours incubation media were removed and a mixture of 100µl TNC assay buffer (50mM Tris, 0.15M NaCl, 10mM $CaCl_2$ and 0.002% NaN_3; pH 7.5) and 100µl of 3µM of the fluorogenic peptide substrate Mca-PLGL-Dpa-AR-NH2 (R&D Systems, Minneapolis, MN) was added per well. After incubation for 1 hour at 37ºC, 20µl of 10X stop solution (100nM EDTA and 0.02% NaN_3; pH 7.5) was added per well. Samples were transferred to a black 96 well microplate and their fluorescence was measured using an excitation wavelength of 325 nm and an emission wavelength of 393 nm, according to the manufacturer´s instructions in a Varioskan Flash spectral scanning multimode reader (Thermo Scientific). For cell-free assays, recombinant human MMP-14 containing the prodomain as well as catalytic and hemopexin domains (Millipore) was activated by incubation with 1mM 4-Aminophenylmercuric acetate (APMA; Sigma) for 2-3 hours at 37ºC. A mixture of 10µl of 200nM MMP-14 solution and 90µl TNC assay buffer was added per well to a black 96-well microplate. After 10 minutes at 37ºC, 100µl of 3µM Mca-PLGL-Dpa-AR-NH2 was added. After incubation during 1 hour at 37ºC 20µl of 10X stop solution was added and fluorescence was measured as above. When necessary, the metalloproteinase activity was determined in the presence of 30µM endoglin peptides or 50µM doxycyclin.

Endoglin peptides and recombinant protein

Short endoglin-related peptides with N-terminal acetylation and C-terminal amidation were synthesized and purified to >90% purity (Biomedal SL, Sevilla, Spain). Peptides P583 (TSKGLVLP) and P230 (GPRTVTVK), corresponding to human endoglin positions 583-590 and 230-237, respectively, were dissolved in distilled water. Peptide P447 (SLSFQLGLYL),

corresponding to human endoglin positions 447-456 was dissolved in 1.6% dimethyl sulfoxide (DMSO). Recombinant human endoglin encoding the extracellular domain (Glu26-Gly586) was purchased from R&D Systems Inc. (Minneapolis, MN, USA; 1097EN).

Mice and in vivo experiments

Mice from the strain C57BL/6J were obtained from The Jackson Laboratory (Bar Harbor, ME, USA). Unless stated otherwise, 8-12 weeks old males were used. A group of four mice were intraperitoneally infused with T09 (40-50mg/kg) or vehicle alone (ethanol-saline solution 1:1) daily during 4-6 days. Longer treatment periods are toxic to the animals due to the ethanol solution. Alternatively, mice were intravenously injected in the tail vein with a liposome mixture containing 22-R (40-50mg/kg) and L-α-phosphatidylcholine at a molar ratio of 1:2, respectively, daily during 4-6 days. The liposome mixture to be injected also contained 60μg/g body weight/day of peptides, as indicated. A subset of animals including 4 pregnant females (20 weeks old, 3rd week of gestation) were injected with liposomes as indicated. Systolic arterial pressure was measured daily during the treatment with a tail cuff sphygmomanometer (NIPREM 546) equipment. Alternatively, systolic arterial pressure was measured by radiotelemetry using a catheter implanted into an artery of the mouse attached to a combination pressure transducer, transmitter and battery, all encapsulated in an implantable microminiaturized electronic monitor (PA-C20, Data Sciences International, DSI; St. Paul, MN, USA). For device implantation in the mice, we have used a technique previously reported.[6,7] Each animal was housed individually in a standard polypropylene cage in a 12:12-h light-dark cycle, fed standard rodent chow, and given drinking water *ad libitum*. At least 3 days after recovery, the cage was placed over a radio receiver and repeated measurements of basal systolic and diastolic arterial pressure and heart rate were performed in each animal between 10:00 a.m. and 14:00 p.m., for at least 10 days to be sure that stable pressures are recorded. Data was digitally recorded on a computer and calculated using the software

provided by Data Sciences. When indicated, blood pressure measurements were performed in anesthetized mice using an intracarotid cannula connected to a blood pressure transducer. At the end of the treatment, animals were sacrificed, plasma was extracted and the levels of murine sEng were determined by ELISA as described above.

The concentration of total protein in urine was measured by a colorimetric assay (Bradford Method). For histological analysis of the kidney, animals were anesthetized with pentobarbital (40 mg/Kg) and perfused with heparinized saline solution followed by 4% buffered formalin. Kidneys were removed, halved longitudinally, fixed for 24 hours in 4% buffered formalin and then embedded in paraffin. Sections, 3 μm thick, were cut and mounted on glass slides and stained with hematoxylin-eosin using standard techniques. All procedures were approved by the Animal Care and Use Committees of the University of Salamanca and mice were cared for in accordance with the standards established in the National Institutes of Health Guide for the Care and Use of Laboratory Animals.

Generation of transgenic mice

To upregulate, in a tetracycline dependent manner, the endogenous MMP-14, Ola129/C57BL/6J knock-in mice were generated. To construct a conditionally regulated allele of MMP-14, a tetracycline-based regulatory cassette was inserted immediately upstream of its translation initiation codon, so that gene expression could be regulated by dietary doxycycline (dox) administration.[8] In this model, the native MMP-14 promoter drives the expression of the binary tetracycline transactivator (tTA) protein, which recognizes the five copies of the tet operator fused to a minimal cytomegalovirus (CMV) promoter (tet_{05}-CMV) leading to the transcription of MMP-14 (Supplementary Fig. 6). In the presence of dox (1 mg/mL) in the drinking water, the binding of tTA to its operator is abolished which in turns blocks the CMV-dependent transcription of the MMP-14. In the absence of dox, MMP-14 expression is increased due to the stronger activity of tet_{05}-CMV promoter versus MMP-14

promoter.[9] For this purpose, a MMP-14-targeting vector was developed by homologous recombination in yeast using the TriTAUBI2 (encoding the tTa, resistance genes Neo and URA flanked with loxP sites, and the tet_{05}-CMV promoter) and Yplac22 (shuttle plasmid) vectors. Two short homology arms (300-bp) immediately upstream and downstream of the translation initiation codon were subcloned into the TriTAUBI2 flanking the tTA-Neo-Ura-tet05CMV-cassette (Supplementary Fig. 6). The resulting construct was cotransformed into yeast with Yplac22 vector containing a 12-kb *EcoRI* genomic DNA fragment encompassing exons 1-8 of MMP-14 gene. After homologous recombination in yeast, the resulting targeting vector was verified by restriction digestion and sequencing, linerized with *NotI* and electroporated into embryonic stem (ES) cells. Resistant clones were selected with G418 antibiotic using conventional procedures, screened by southern-blot following *EcoRV* digestion of genomic DNA and hybridized with a radiolabeled 5'-external probe (Supplementary Fig. 6). A 21-kb fragment was detected from the wild-type allele and a 12.5-kb fragment from the targeted (Tg) alelle. Recombinant clones were confirmed using the 5´-external probe. Germline transmitting chimeras were created by aggregation in morulas. Chimeric mice were bred with C57BL/6J females and the offspring heterozygous were mated to Sox2-Cre transgenic mice in order to deplete de Ura-Neo cassette. Mice genotypes were determined by southern-blot analysis of tail DNA. The conditionally regulated animals are viable in the presence of dox. In this work, the upregulation of MMP-14 was induced when mice were 5 weeks old.

To generate a transgenic mice expressing soluble endoglin (*sol.Eng*$^{+}$), an endoglin expression construct was obtained by inserting the endoglin cDNA into plasmid pCAGGS (10) in a modified version for mouse transgenesis.[11] This plasmid contains, from 5´ to 3´, a CMV enhancer, a chicken enhancer and promoter, a β-globin intron, an *EcoRI* site, and a β-globin polyadenylation motif.[11] HA-tagged human endoglin cDNA in pDisplay[12] was used to derive

by PCR a truncated endoglin construct encoding the orphan domain and the ZP-N domain (amino acids 26-437). The 1.3-kb PCR product was cloned into pCR®II-TOPO (Invitrogen). The resulting vector was digested with *EcoR I*, and the endoglin fragment was inserted into the *EcoRI* site of the pCAGGS plasmid under the control of a ubiquitous actin promoter. The expression vector was digested with *SalI*/*KpnI* and the endoglin containing 4.2-kb fragment was separated by agarose gel electrophoresis. The purified fragment was microinjected into CBAxC57BL/6J fertilized eggs at the University of Salamanca Transgenic Facility, using standard protocols. Progeny was screened for endoglin transgene by PCR of tail DNA using a forward primer specific for the pDisplay leader sequence (5´-GGGGATATCCACCATGGAGA -3´) and a reverse primer of human endoglin (5´-TGCAGGAAGACACTGCTGTTTAC -3´). Transgenic founders were crossed with CD1 x C57BL/6J hybrids to perpetuate the transgenic lines. Three independent transgenic founders were generated showing similar phenotypic features in all the derived transgenic lines. Studies reported here were performed in the F7 generation.

In MMP-14 and endoglin transgenic animals and in their wild type (WT) littermates, plasma was extracted from a tail tip cut by capillary centrifugation and the levels of human sEng were determined by ELISA.

Statistics

Data were subjected to statistical analysis and results are shown as mean ±SEM. Differences in mean values between two groups were analyzed using Student's *t*-test (unpaired). Comparisons of several groups were done by one way (a single variable) or two-way (two variables) ANOVA. Then, a posteriori *t*-test was used for group comparison (GraphPad Software).

REFERENCES

1. Letamendía A, Lastres P, Almendro N, Raab U, Bühring HJ, Kumar S, Bernabéu C. Endoglin, a component of the TGF-beta receptor system, is a differentiation marker of human choriocarcinoma cells. *Int J Cancer.* 1998;76:541-546.

2. Letamendía A, Lastres P, Botella LM, Raab U, Langa C, Velasco B, Attisano L, Bernabeu C. Role of endoglin in cellular responses to transforming growth factor-beta. A comparative study with betaglycan. *J Biol Chem.* 1998;273:33011-33019.

3. Bellón T, Corbí A, Lastres P, Calés C, Cebrián M, Vera S, Cheifetz S, Massague J, Letarte M, Bernabéu C. Identification and expression of two forms of the human transforming growth factor-beta-binding protein endoglin with distinct cytoplasmic regions. *Eur J Immunol*. 1993;23:2340-2345.

4. Guerrero-Esteo M, Sanchez-Elsner T, Letamendia A, Bernabeu C. Extracellular and cytoplasmic domains of endoglin interact with the transforming growth factor-beta receptors I and II. *J Biol Chem.* 2002;277:29197-29209.

5. Bligh EG, Dyer WJ. A rapid method of total lipid extraction and purification. *Can J Biochem Physiol.* 1959;37:911-917.

6. Blanco FJ, Grande MT, Langa C, Oujo B, Velasco S, Rodriguez-Barbero A, Perez-Gomez E, Quintanilla M, López-Novoa JM, Bernabeu C. S-endoglin expression is induced in senescent endothelial cells and contributes to vascular pathology. *Circ Res*. 2008;103:1383-1392.

7. Grande MT, Pascual G, Riolobos AS, Clemente-Lorenzo M, Bardaji B, Barreiro L, Tornavaca O, Meseguer A, López-Novoa JM. Increased oxidative stress, the renin-angiotensin system, and sympathetic overactivation induce hypertension in kidney androgen-regulated protein transgenic mice. *Free Radic Biol Med*. 2011;51:1831-1841.

8. Bond CT, Sprengel R, Bissonnette JM, Kaufmann WA, Pribnow D, Neelands T, Storck T, Baetscher M, Jerecic J, Maylie J, Knaus HG, Seeburg PH, Adelman JP. Respiration and parturition affected by conditional overexpression of the Ca^{2+}-activated K^{+} channel SK3. *Science*. 2000;289:1942-1946.

9. Hayakawa T, Yusa K, Kouno M, Takeda J, Horie K. Bloom's syndrome gene-deficient phenotype in mouse primary cells induced by a modified tetracycline-controlled trans-silencer. *Gene*. 2006;369:80-89.

10. Niwa H, Yamamura K, Miyazaki J. Efficient selection for high-expression transfectants with a novel eukaryotic vector. *Gene*. 1991;108:193-199.

11. del Mar Lorente M, Marcos-Gutiérrez C, Pérez C, Schoorlemmer J, Ramírez A, Magin T, Vidal M. Loss- and gain-of-function mutations show a polycomb group function for Ring1A in mice. *Development*. 2000;127:5093-5100.

12. Guerrero-Esteo M, Sanchez-Elsner T, Letamendia A, Bernabeu C. Extracellular and cytoplasmic domains of endoglin interact with the transforming growth factor-beta receptors I and II. *J Biol Chem*. 2002;277:29197-29209.

LEGENDS TO SUPPLEMENTARY FIGURES

Supplementary Figure 1. Analysis of cholesterol and 22-R-hydroxycholesterol in cellular extracts. Lipids were analyzed by gas chromatography-mass spectrometry (GC-MS) using the Agilent 7890A equipment (Agilent Technologies). In Panels **A-D** the horizontal axis represents the time of elution, while the vertical axis displays the intensity of the signal in picoamperes (pA). Panel **A** shows the profile of the solvent (Vehicle), while panel **B** shows the two control markers, purified cholesterol and 22-R. In panels **C** and **D** lipid extracts from JAR cells, incubated under normoxia or hypoxia for 24 hours, were subjected to GC-MS. The time of elution and position of cholesterol and 22-R peaks are indicated. The area of these peaks was measured in three different experiments and the mean is depicted in panel **E**. The levels of 22-R in JAR cells subjected to hypoxia displayed a marked increase (~4-fold induction) respect to normoxic cells; differences were assessed by *t*-test (n=3 in each group). Identification of the peaks obtained by GC-MS was confirmed by the information available in the MS databases,.

Supplementary Figure 2. Effect of LXR ligands on endoglin expression. JAR cells were incubated with T09, RA, 22-R or vehicle (0.1% ethanol in culture medium) for 24 hours, as indicated. Then, cells were harvested and cell surface endoglin was measured by flow cytometry (**A** and **B**), while the corresponding culture supernatants were saved for soluble endoglin measurements (see Fig. 2). **A.** Flow cytometry analysis. Cells were analyzed by immunofluorescence flow cytometry with anti-endoglin mAb P4A4, using as a negative control the mAb X63. The percentage of positive cells and the mean fluorescence intensity are indicated. **B**. Expression index of membrane bound endoglin (mEng) was calculated using data from panel **A** by multiplying the positive cell percentage by the mean fluorescence intensity of each sample. **C**. Comparative induction by LXR ligands of soluble endoglin

(sEng) versus membrane bound endoglin (mEng). The ratio of mEng expression index (**B**) and sEng (Figure 2) were calculated and an arbitrary value of 1 was assigned to the untreated sample (CTL). A marked increase of the sEng/mEng ratio was observed upon treatment with LXR ligands.

Supplementary Figure 3. Effect of LXR ligands and hypoxia on MMP-14 expression. JAR cells were incubated with T09, RA, 22-R, vehicle (0.1% ethanol in culture medium), 1% O_2 (hypoxia), and 21% O_2 (normoxia) for 24 hours, as indicated. Cells were harvested and cell surface MMP-14 was measured by immunofluorescence flow cytometry with a rabbit anti-MMP-14 mAb (EP1264Y), using a negative control antibody. The percentage of positive cells and the mean fluorescence intensity are indicated. An increased expression of MMP-14 was observed upon treatment with LXR ligands.

Supplementary Figure 4. Diastolic and mean arterial pressure in oxysterol-treated and *Sol.eng*$^+$ transgenic mice. **A** and **B**. Effect of LXR ligands on diastolic and mean arterial pressure. Male mice were intravenously injected daily with 22-R or vehicle (CTL). During treatment, the systolic, diastolic and mean arterial pressure was measured daily by telemetry. Measurements of the diastolic arterial pressure (**A**) and mean arterial pressure (**B**) are shown. Analysis by two-way ANOVA with one fixed factor (treatment) and repeated measures (time); for every time point the *t*-test was made (control vs treatment). In panel **A**, there is statistical difference from day 2 between 22R and control group (*t*-test, confidence level=0.001 in day 2 and 0.005 in day 3; ***P<0.001; **P<0.0086). In panel **B**, from day 2 of treatment there is a statistical difference between 22R and control group (*t*-test, confidence level=0.005; ***P<0.001). The corresponding systolic arterial pressure is in Figure 5B. **C** and **D**. Diastolic (**C**) and mean (**D**) arterial pressure was measured by telemetry in wild type (WT) and *Sol.eng*$^+$ transgenic male mice. Differences between groups were assessed by two-way ANOVA followed by *t*-test. The number (n) of animals used in each condition is indicated.

Supplementary Figure 5. Effect of LXR ligands on protenuria. Male mice were intravenously injected daily with 22-R or vehicle (Control) for three days. During treatment, the systolic arterial pressure was measured daily by telemetry (Figure 5B). The last day of treatment, mice urine samples were collected. The concentration of total protein in urine was measured by a colorimetric assay (Bradford Method). The number (n) of animals used is indicated, differences were assessed by *t*-test.

Supplementary Figure 6. Schematic representation of the conditionally regulated MMP-14 allele and the theory of the gene switch. The regulatory cassette was inserted immediately upstream of the translational initiation site of MMP-14. The drawing is not to scale.

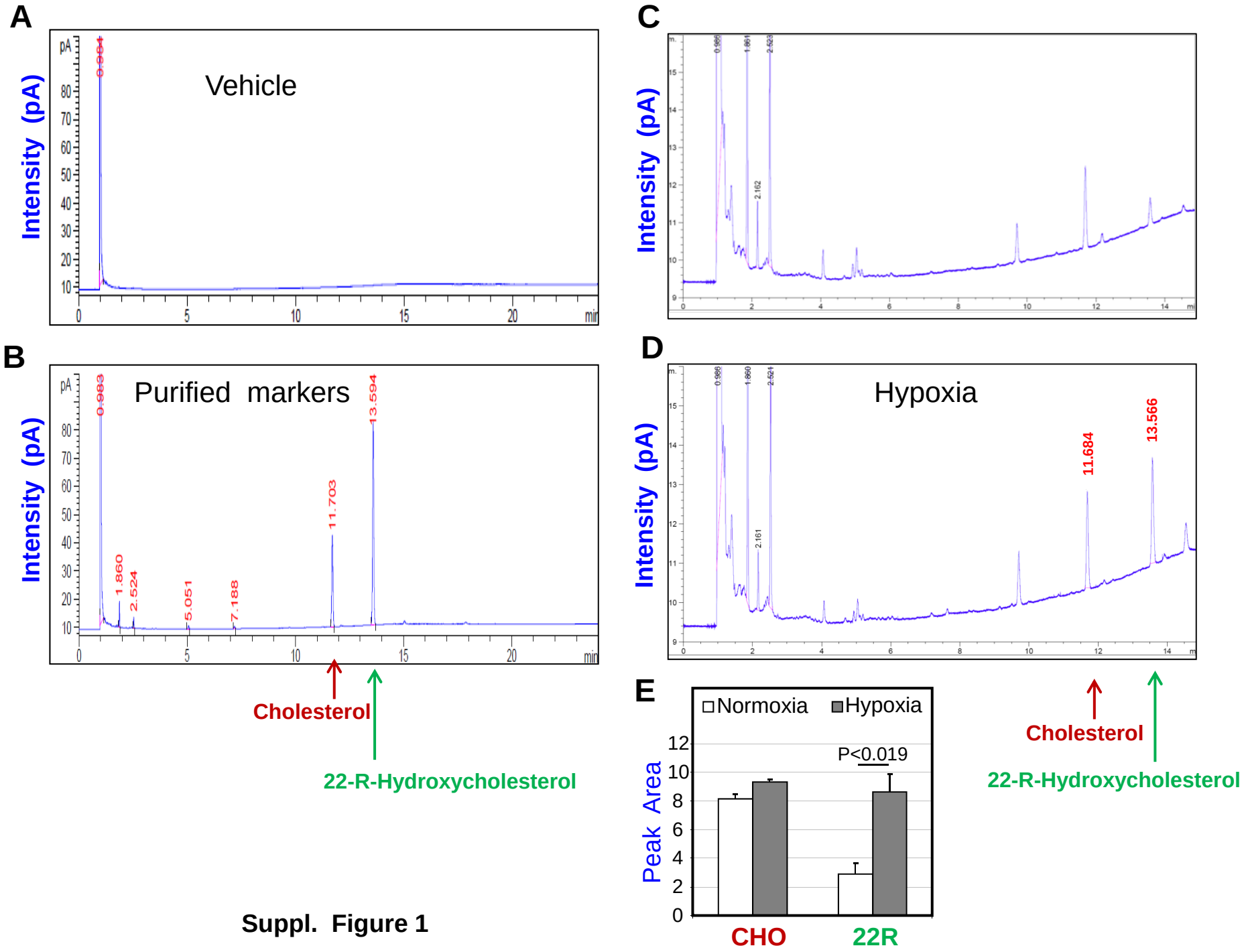

Suppl. Figure 1

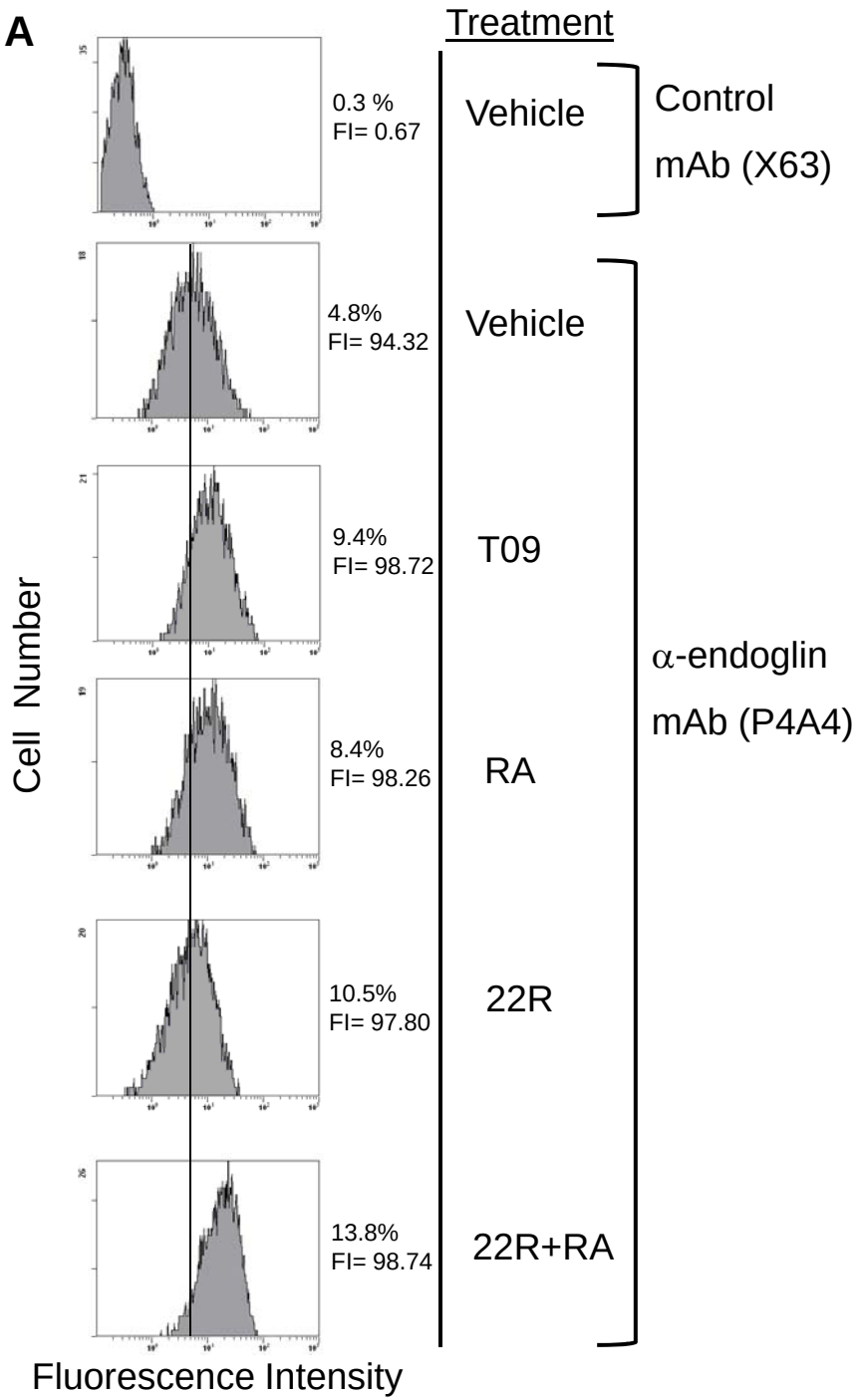

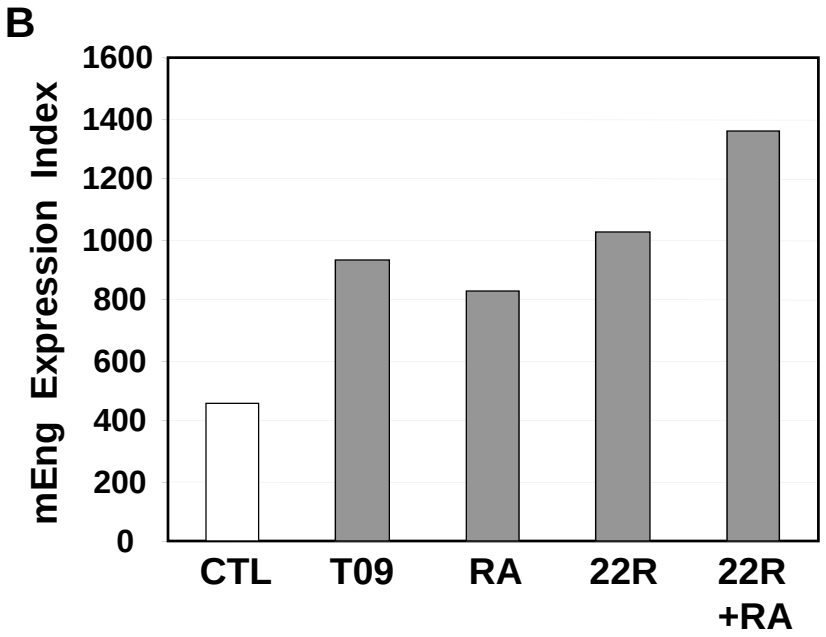

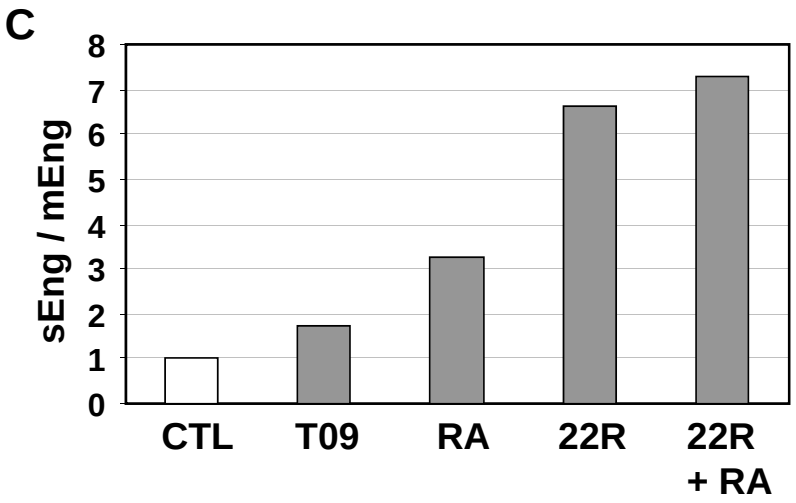

Suppl. Figure 2

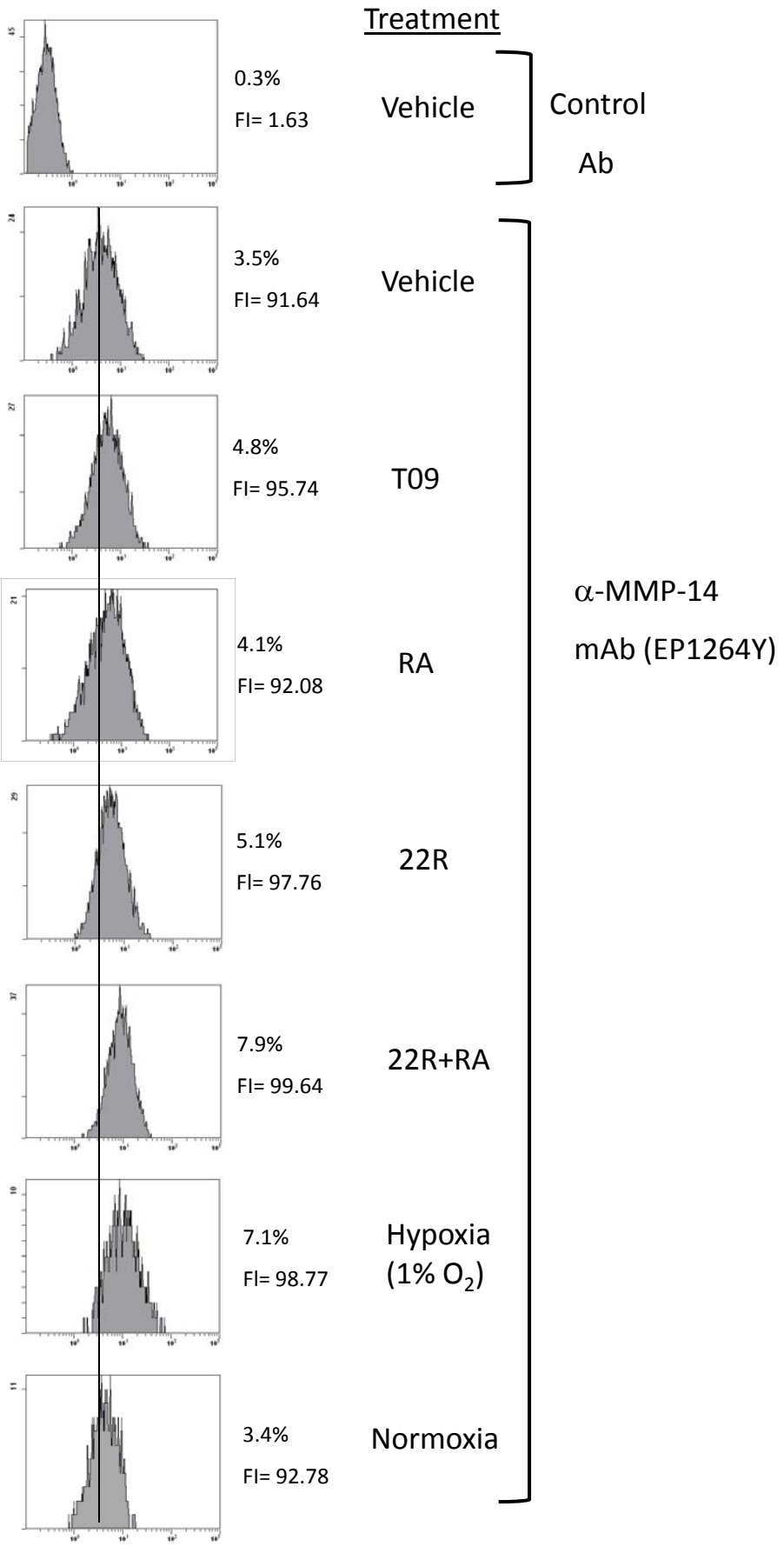

Suppl. Figure 3

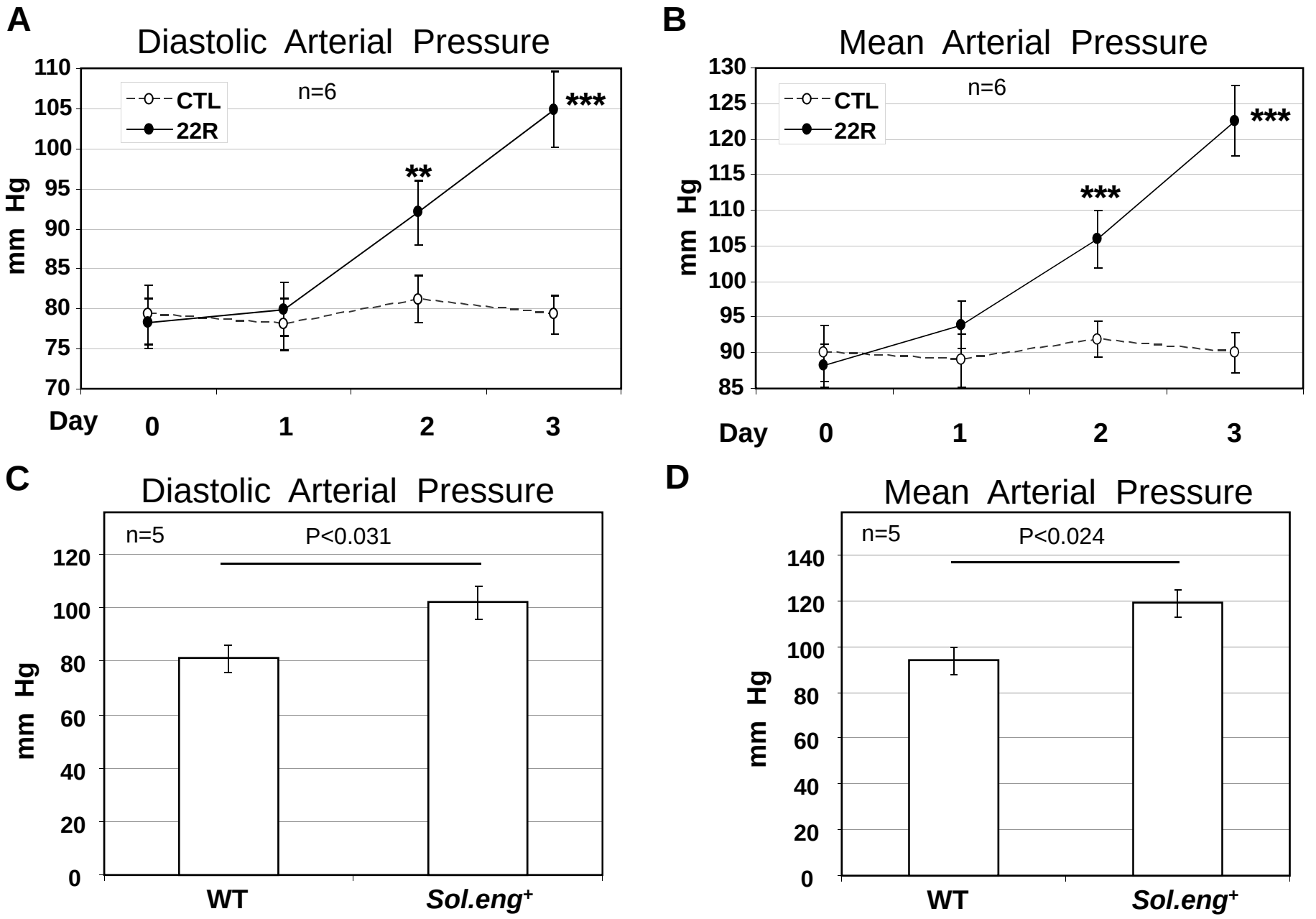

Suppl. Figure 4

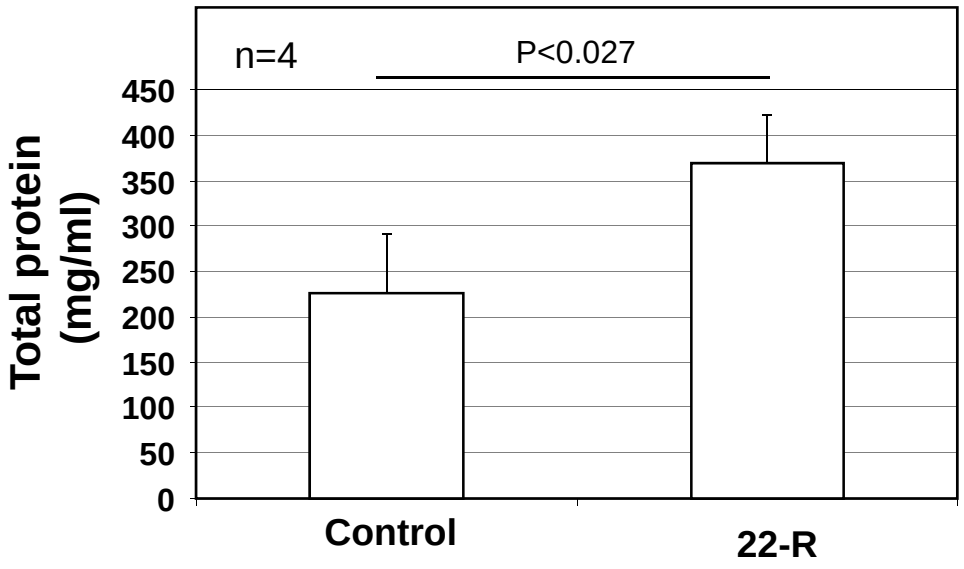

Suppl. Figure 5

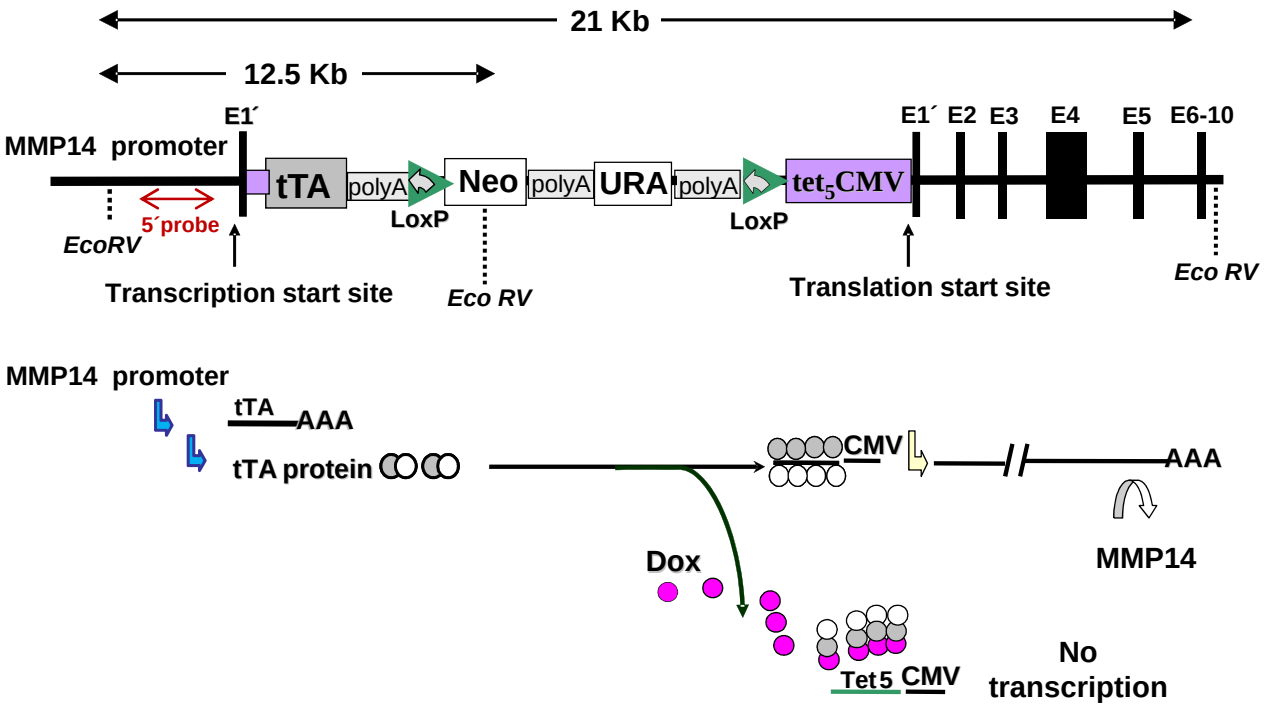

Suppl. Figure 6